

MICROCOPY RESOLUTION TEST CHART
NATIONAL BUREAU OF STANDARDS-1963-A

ARL-MECH-ENG-NOTE-386

AR-002-269



LEVEL

AD A108254

DEPARTMENT OF DEFENCE
DEFENCE SCIENCE AND TECHNOLOGY ORGANISATION
AERONAUTICAL RESEARCH LABORATORIES
MELBOURNE, VICTORIA

MECHANICAL ENGINEERING NOTE 386

PERFORMANCE ANALYSIS OF VAPOUR CYCLE
COOLING SYSTEMS

by

BRIAN REBBECHI
JOHN L. FOWLER
NEIL J. REPACHOLI
GORDON L. COLLINS

Approved for Public Release.

DTIC
ELECTE
DEC 9 1981
S D

© COMMONWEALTH OF AUSTRALIA 1981

COPY No 18

MARCH 1981

81 12 08286

DTIC FILE COPY

AR-002-269

DEPARTMENT OF DEFENCE
DEFENCE SCIENCE AND TECHNOLOGY ORGANISATION
AERONAUTICAL RESEARCH LABORATORIES

MECHANICAL ENGINEERING NOTE 386

**PERFORMANCE ANALYSIS OF VAPOUR CYCLE
COOLING SYSTEMS**

by

BRIAN REBBECHI
JOHN L. FOWLER
NEIL J. REPACHOLI
GORDON L. COLLINS

SUMMARY

The performance of several different configurations of vapour cycle cooling systems, using automotive-type components, has been experimentally determined.

Performance of the individual components has also been analysed and presented in a form appropriate for assessing the suitability of their application to other system types.



POSTAL ADDRESS: Chief Superintendent, Aeronautical Research Laboratories,
Box 4331, P.O., Melbourne, Victoria, 3001, Australia.

DOCUMENT CONTROL DATA SHEET

Security classification of this page: Unclassified

1. Document Numbers (a) AR Number: AR-002-269 (b) Document Series and Number: Mechanical Engineering Note 386 (c) Report Number: ARL-Mech-Eng-Note-386	2. Security Classification (a) Complete document: Unclassified (b) Title in isolation: Unclassified (c) Summary in isolation: Unclassified														
3. Title: PERFORMANCE ANALYSIS OF VAPOUR CYCLE COOLING SYSTEMS															
4. Personal Authors: Rebbechi, B. Fowler, J. L. Repacholi, N. J. Collins, G. L.	5. Document Date: March, 1981														
6. Type of Report and Period Covered:															
7. Corporate Author(s): Aeronautical Research Laboratories	8. Reference Numbers (a) Task: NAV 77/018 (b) Sponsoring Agency: Department of Defence (Navy Office)														
9. Cost Code: 43 4310															
10. Imprint: Aeronautical Research Laboratories, Melbourne	11. Computer Programs (Titles and languages):														
12. Release Limitations (of the document): Approved for public release															
12.0 Overseas:															
<table border="1"> <tr> <td>N.O.</td> <td></td> <td>P.R.</td> <td>1</td> <td>A</td> <td></td> <td>B</td> <td></td> <td>C</td> <td></td> <td>D</td> <td></td> <td>E</td> <td></td> </tr> </table>		N.O.		P.R.	1	A		B		C		D		E	
N.O.		P.R.	1	A		B		C		D		E			
13. Announcement Limitations (of the information on the page): No limitations															
14. Descriptors: Cooling systems Air conditioners Aircraft cabins Automobiles	15. Cosati Codes: 1301 0103 1306														
Dichlorodifluoromethane Refrigerants Environmental control systems															

16. **ABSTRACT**

The performance of several different configurations of vapour cycle cooling systems, using automotive-type components, has been experimentally determined.

Performance of the individual components has also been analysed and presented in a form appropriate for assessing the suitability of their application to other system types.

Accession For	
NTIS GRA&I	<input checked="" type="checkbox"/>
DTIC TAB	<input type="checkbox"/>
Unannounced	<input type="checkbox"/>
Justification	
By	
Distribution/	
Availability Codes	
Dist	Avail and/or Special
A	

DTIC
ELECTE
S DEC 9 1981 D
D

CONTENTS

	Page No.
1. INTRODUCTION	1
2. PERFORMANCE TESTS OF COMPLETE AUTOMOTIVE EVAPORATOR ASSEMBLIES	1
2.1 Description of Cooling System	1
2.2 Test Results of Single Imperial 5 Evaporator Assembly	2
2.3 Test Results of Cooling System Using Two Parallel Imperial 5 Evaporator Assemblies	2
3. PERFORMANCE TESTS OF GENERAL AUTOMOTIVE-TYPE COOLING SYSTEM COMPONENTS	2
3.1 Description of Cooling System	2
3.2 Test Results	3
3.3 Discussion	3
3.3.1 Cooling Capacity	3
3.3.2 Compressor Power Consumption	4
3.3.3 Coefficient of Performance	4
3.3.4 Compressor Isentropic Efficiency	4
3.3.5 Compressor Volumetric Efficiency	4
3.3.6 Cooling Capacity Change with Varying Evaporator Air Inlet Temperature	4
4. PERFORMANCE OF INDIVIDUAL COMPONENTS	5
4.1 Compressor Performance	5
4.2 Evaporator Performance	5
4.3 Condenser Performance	5
5. COMPONENT BALANCING IN COOLING SYSTEMS	5
6. DISCUSSION	6
REFERENCES	
ACKNOWLEDGEMENT	

APPENDICES

- 1. Test Results for Cooling System with Single Imperial 5 Evaporator Assembly**
- 2. Test Results for Cooling System with Two Parallel Imperial 5 Evaporator Assemblies**
- 3. Cooling System Test Results**
- 4. Test Results with Varying Evaporator Inlet Air Temperature**
- 5. Data Points for Compressor Performance Characteristics**
- 6. Data Points for Extension of Evaporator Performance Characteristics**

FIGURES

DISTRIBUTION

1. INTRODUCTION

Vapour cycle systems are widely used in industrial and domestic cooling equipment. However, their application to aircraft cabin cooling is very limited, particularly with regard to aircraft operating in Australia. The interest of ARL in vapour cycle cooling systems arose in part from the general requirements of Task No. AIR-71/14, Cockpit Conditioning, and more particularly because of problems of excessive cabin temperatures encountered by the Royal Australian Navy during operation of Sea King Mk. 50 Helicopters (described by Rebbechi and Edwards 1979).

In view of the likely future involvement of ARL with vapour cycle cooling systems, it was decided to carry out bench testing of automotive-type air conditioning components. These automotive components were selected primarily because of their low cost, relatively light weight, and ready availability. Also it was known that these components were used in light aircraft cooling systems. More specialised complex components, such as hermetically sealed rotary compressor-motor units and light-weight heat exchangers, were used in larger aircraft where cost was a less important factor and system capacity requirements greater.

The aims of the initial test programme were to:

- (a) gain general experience with vapour cycle systems;
- (b) establish the performance characteristics of the components and so gain an accurate appreciation of the size, weight and power requirements for particular cooling loads.

The aims of the initial programme were subsequently varied to include the more specific requirement to develop a system with a cooling capacity of 10 kW, which could be used as a trial installation in the Sea King Helicopter. A description of the cooling system subsequently constructed at ARL and installed in the Sea King is given by Rebbechi (1980).

This report summarises the results obtained from bench tests of the basic cooling system, and analyses the performance of the individual components, namely the compressor, evaporator and condenser. Two series of tests were undertaken. The first series used complete automotive evaporator assemblies (that is evaporators complete with 12-volt fan for air reticulation); the second used larger evaporators mounted in a duct with variable air supply.

2. PERFORMANCE TESTS OF COMPLETE AUTOMOTIVE EVAPORATOR ASSEMBLIES

2.1 Description of Cooling System

A schematic diagram of the cooling system is given in Figure 1. The control valves shown enabled separate or combined testing of the evaporators. The evaporator assemblies used at this stage of the tests were automotive types designed for mounting in the vehicle cabin. A complete evaporator assembly is shown in Figure 2; the evaporator matrix is shown separately in Figure 3. An airflow calibration of the evaporator and 12-volt fan assembly, with and without air-grille mounted, is given in Figure 4. The evaporator matrix dimensions and construction are illustrated in Figure 5. The condenser is pictured in Figure 6a; the dimensions are given in Figure 6b.

The refrigerant compressor used was a Sankyo SD-508 (Fig. 7) intended for use in automotive air conditioning systems. It is, at times, mistakenly termed a 'rotary' compressor, but is actually a 5-cylinder swashplate type. The power consumption was measured by mounting the compressor in a cradle pivoting about an axis co-incident with the axis of rotation of the compressor pulley, and measuring the reaction torque by means of a load cell and moment arm. The speed was measured by a stroboscope.

The refrigerant used for these and all subsequent tests was dichlorodifluoromethane, commonly termed R12 or Freon 12. This refrigerant is non-flammable and non-toxic, and is used for most automotive and aircraft applications.

2.2 Test Results of Single Imperial 5 Evaporator Assembly

The results of two tests using a single evaporator assembly are given in detail in Appendix 1. A summary of the results is given in Table 1.

TABLE 1
Test Results of a Single Imperial 5 Evaporator

Test No.	Compressor speed (r/min)	Evaporator inlet air temp. (°C)	Condenser inlet air temp. (°C)	Compressor power (kW)	Cooling effect (kW)	Coefficient of performance	Compressor isentropic efficiency
1	2713	34.0	34.5	2.47	3.80	1.54	0.74
2	2713	21.6	20.5	2.57	3.67	1.43	0.69

A typical pressure-enthalpy (Mollier) diagram for a complete refrigeration cycle is illustrated in Figure 8. The pressure-enthalpy diagram for test 2 is illustrated in Figure 9. As no measurement of refrigerant mass flow was made for these particular tests, this diagram cannot be directly correlated with that section of the performance data which contains rate information (such as cooling effect and motor power). The compressor isentropic efficiency, as given in Table 1, can be found by reference to the refrigerant states at inlet and outlet of the compressor.

2.3 Test Results of Cooling System Using Two Parallel Imperial 5 Evaporator Assemblies

The system used for these tests was as shown in the schematic diagram of Figure 1, with both evaporator isolating valves fully opened, and the evaporator outlet air-grilles removed. The results of three tests are summarised in Table 2, and presented in detail in Appendix 2. The pressure-enthalpy diagram for Test 5 is given in Figure 9.

TABLE 2
Test Results Using Two Parallel Imperial 5 Evaporator Assemblies

Test No.	Compressor speed (r/min)	Evaporator inlet air temp. (°C)	Condenser inlet air temp. (°C)	Compressor power (kW)	Cooling effect (kW)	Coefficient of performance	Compressor isentropic efficiency
3	2713	23.0	21.6	2.46	5.12	2.04	0.72
4	2713	24.5	22.5	2.46	5.48	2.21	0.71
5	2713	34.6	33.8	3.24	5.33	1.64	0.77

3. PERFORMANCE TESTS OF GENERAL AUTOMOTIVE-TYPE COOLING SYSTEM COMPONENTS

3.1 Description of Cooling System

A schematic diagram of the cooling system is given in Figure 10. An overall view of the cooling system rig is given in Figure 11; the two parallel evaporators were duct-mounted (Fig. 12) and sited in a separate room in which the air temperature could be controlled by electrical heaters. The mass flow of air through the evaporators was adjusted by varying the fan speed.

The refrigerant compressor was a York 209 twin-cylinder reciprocating piston compressor (Fig. 13) having a displacement of 142 cm^3 (8.7 in^3) per revolution; a variable speed (0–3000 r/min) drive was provided. The compressor was mounted in a cradle (Fig. 14) and the power consumption measured as for the earlier tests described in Section 2, except for the use of a spring balance for measuring reaction torque.

The condenser assembly used for these tests comprised three automotive type UC1C condensers connected in parallel (Fig. 15). This arrangement was selected because of its ready availability at the time of the tests. However, it is not considered by the authors to be the most ideal arrangement because:

- (a) the three refrigerant processes pertaining to the operation of the condenser, that is desuperheating, condensing and subcooling cannot be directed to the most appropriate region of the condenser matrix. To maximise heat exchanger effectiveness, desuperheating should take place in the leaving airstream and subcooling in the entering airstream. Common practice is to situate a subcooling coil in the airstream entering the condenser.
- (b) Subcooling takes place in the lower part of the condenser, which also acts as a liquid receiver; however changes in evaporator cooling requirements can cause the liquid level to build up thereby reducing the cooling capacity.

A preferable (and usual) arrangement is depicted in Figure 16. It should be appreciated that the 'receiver' in Figure 10 only fulfils the requirements for a liquid receiver (that is to absorb fluctuations in liquid refrigerant requirements) when there is no liquid refrigerant in the condenser.

An oil separator was originally installed in the compressor discharge line, however it was subsequently removed because of unresolved problems of excessive refrigerant return to compressor inlet. Thus the volume flow rate (measured by turbine flow meter) in the liquid refrigerant line included a contribution due to compressor oil carry-over.

3.2 Test Results

Results have been analysed from a series of twenty-seven test runs covering all the combinations of three compressor speeds (1000, 2000, 3000 r/min), three compressor discharge pressures (nominally 1030, 1380, 1720 kPa gauge) and three evaporator airflows. Inlet air temperature was nominally constant at 30°C . These results, summarised in Appendix 3, include the system coefficient of performance, and the volumetric and isentropic efficiencies of the compressor.

The compressor isentropic efficiency was calculated from the refrigerant states at inlet and outlet, and the volumetric efficiency from the mass flow and refrigerant state at entry to the compressor. From the results in Appendix 3, graphs have been plotted of cooling capacity, compressor power consumption, coefficient of performance, isentropic and volumetric efficiencies, versus compressor speed. These graphs are given in Figures 17–21.

Additional tests were carried out at constant compressor speed (2000 r/min) and nominally constant compressor discharge pressure (1650 kPa gauge) to determine the effect of varying the evaporator inlet air temperature. The results from these tests are summarised in Appendix 4, and in Figure 22 the change in cooling capacity with evaporator inlet air temperature is plotted.

3.3 Discussion

3.3.1 Cooling Capacity

The cooling capacity of the system is considerably influenced by compressor speed and evaporator airflow, but the effect of compressor discharge pressure is small (Fig. 17). Cooling capacity increases with compressor speed but at a decreasing rate due to deteriorating compressor volumetric efficiency. This effect is particularly apparent at moderate evaporator airflows.

3.3.2 Compressor Power Consumption

The compressor power consumption (Fig. 18) increased with increasing compressor speed as expected, and reached a maximum of 4.6 kW. The power requirement referred to here is measured at the compressor and does not include drive losses. Other (unrelated) tests have shown that vee-belt drive losses of 10–20% can be encountered in some circumstances, depending on pulley diameters and number of belts.

3.3.3 Coefficient of Performance

The coefficient of performance (COP) of the cooling system, defined by the ratio of cooling capacity to input power, is plotted in Figure 19. The COP may be as high as 4.1 (Fig. 19a), however this value is not considered truly representative as here the compressor speed is low (1000 r/min) and the evaporator airflow high. Reference to this particular test (Appendix 3, test No. 19) shows that the difference between condensing and evaporating temperatures is smaller than for any of the other tests, thus the COP, which is given theoretically by

$$\text{COP} = T_b (T_a - T_b),$$

where T_a is the upper temperature and T_b the lower temperature, would be expected to be quite high.

A more typical COP for this system would be 2–2.5 (Figs. 19b, c). This COP does not include compressor motor and drive inefficiencies, and power requirements of the evaporator and condenser fans. When these additional power requirements are included, the overall COP will fall to about unity, as found for the cooling system built for the Sea King Helicopter (Rebbechi 1980).

3.3.4 Compressor Isentropic Efficiency

The isentropic efficiency (Fig. 20) ranges from 0.70 to 0.94 and, as expected, decreases with increasing compressor speed, presumably due to losses through the compressor reed valves and ports.

3.3.5 Compressor Volumetric Efficiency

The compressor volumetric efficiency (Fig. 21) ranges from 0.84 (at low speed, low discharge pressure) to 0.46 (at high speed, high discharge pressure). This rapid decrease in efficiency with increasing compressor speed was unexpected, as data of this form was not available prior to testing of these components. The refrigerant compressor used for these tests has a speed limitation (set by the manufacturer) of 6000 r/min for safe operation. However, due to the deterioration of volumetric efficiency, there is little advantage in using high rotational speeds to achieve increased cooling capacity. The high speed capability of 6000 r/min is necessary where the compressor is directly driven from a motor vehicle engine; a high level of cooling is usually required at low engine speeds (particularly at idle) and the decrease in volumetric efficiency at high speeds is a useful power limiting characteristic, obviating the necessity for providing additional controls on the cooling system to limit the compressor mass flow.

3.3.6 Cooling Capacity Change with Varying Evaporator Air Inlet Temperature

Figure 22 shows that the system cooling capacity increases markedly with increasing evaporator inlet air temperature—from 4 kW at 15°C to 8 kW at 40°C. The main factors influencing this trend are improved evaporator heat transfer and increased refrigerant mass flow (due to higher suction pressures).

4. PERFORMANCE OF INDIVIDUAL COMPONENTS

The foregoing Sections 2 and 3 describe the performance of particular complete cooling systems. However, mutual interaction between components tends to mask knowledge of their individual performance. This section examines the performance of the components when considered as separate entities so that the behaviour of, for example, the compressor when applied to any given system, can be assessed.

4.1 Compressor Performance

The cooling capacity of the York 209 compressor is given in Figures 23–25 for three speeds (1000, 2000, 3000 r/min), and is plotted versus condensing temperature for various values of suction saturation temperature. The compressor power consumption, similarly presented, is given in Figure 26. The data from which these figures are derived are given in Appendix 5. As the degree of subcooling in the system on test was much higher than is achieved in normal installations, the cooling capacity data of Appendix 3 has been corrected, where necessary, for 6°C of subcooling only. Details of the corrections are given in Appendix 5.

The compressor performance diagrams (Figs. 23–26) could alternatively have been plotted in terms of compressor discharge pressure (in place of condensing temperature) and compressor suction pressure (in place of suction saturation temperature). However, the reference to temperature is compatible with the usual format for evaporator and condenser performance diagrams.

4.2 Evaporator Performance

Details of a single evaporator matrix are given in Figure 27. The performance characteristics (Fig. 28) refer to the dual arrangement of Figure 10; the performance of each evaporator individually is obtained by halving the cooling capacities plotted. Additional tests (Appendix 6) were undertaken at low compressor speed (515 r/min) to provide data in the low cooling capacity region of these curves.

The characteristics presented are for dry operation of the evaporator and show the effect of varying inlet air *dry bulb* temperature. Where the evaporator function includes dehumidification in addition to cooling, the effect of inlet air *wet bulb* temperature is more appropriate.

4.3 Condenser Performance

The condenser performance is given in Figure 29 for one cooling air mass flow. This performance diagram is for the three parallel-connected condensers, as illustrated in the schematic of Figure 10. The condensers were placed in series in the cooling airstream. One of the condensers, which was manufactured for automotive use, is pictured in Figure 30. As has been discussed in Section 3.1, this condenser arrangement is not considered ideal but was utilised only because more suitable components were not available.

The condenser performance (Fig. 29) was found from the data of Appendix 3. Interpolation has been necessary as the data showed considerable variability, thought to be caused primarily by a changing liquid level in the condensers. Such a change would alter the area available for heat transfer in the desuperheating and condensing phases, and hence alter the overall heat transfer coefficient for the condenser. In addition the liquid level in each of the three condensers may have differed, so that the performance capability of a single condenser may not simply be one-third of the heat rejection capability of Figure 29.

5. COMPONENT BALANCING IN COOLING SYSTEMS

The performance of the compressor, evaporator and condenser operating together can be found by eliminating the internal variables, namely the condensing temperature and suction saturation temperature. The system performance can then be described in terms of the external variables—the evaporator and condenser entering air temperatures and velocities, and the

compressor speed. This solution could be obtained analytically, by expressing the component characteristics as algebraic equations and simultaneously solving these, or by employing digital computer techniques. A rather simpler graphical method as described in detail by the American Society of Heating, Refrigerating and Airconditioning Engineers (1965) can suffice; a brief description is given here.

Consider, for example, a compressor speed of 2000 r/min. Superimpose the condenser characteristics of Figure 29 onto the curves giving required condenser heat rejection (Figure 24b) to give the combined plot, for compressor and condenser, illustrated in Figure 31b. Transfer the points of intersection on this plot to the corresponding suction saturation temperature curves of Figure 31a. There now result the cooling capacity and condensing temperatures arising from operation of this particular compressor/condenser combination. Figure 31a can then be replotted on the evaporator performance diagram (using, for example, the high evaporator airflow characteristic, Figure 28a), resulting in Figure 32a. The points of intersection of lines on Figure 32a can then be replotted, resulting in the overall system performance diagram of Figure 32b. The effects of pressure drop have been neglected here; these can be considered by converting to an equivalent temperature drop, and adjusting the superposition of the curves accordingly.

The advantages of using digital computer techniques for the design of systems to cover *differing* requirements is obvious—optimisation of component sizes (including fans for condenser/compressor airflow) can then readily be carried out.

6. DISCUSSION

At the outset of this programme very little quantitative data was available relating to the performance of the components of automotive-type cooling systems. For this reason a detailed analysis and description of the individual components has been provided in this report; by extrapolation, this description should enable estimation of the performance of other similar automotive-type components.

Unlike the evaporator and condenser, for which no performance characteristics were available, published compressor characteristics were readily obtainable from the suppliers. These, however, were found to be rather more optimistic with regard to cooling capacity than the results obtained from these tests. There is no obvious reason for this discrepancy.

REFERENCES

- American Society of Heating, Refrigerating and Airconditioning Engineers (1965). *ASHRAE Guide and Data Book, Fundamentals and Equipment*. New York: American Society of Heating, Refrigerating and Airconditioning Engineers, Inc.
- Rebbechi, B. (1980). *A Vapour Cycle Cabin Cooling System for the Sea King Mk. 50 Helicopter*. Mech. Eng. Rep. 155. Feb. 1980. Melbourne: Aeronautical Research Laboratories.
- Rebbechi, B., and Edwards, D. H. (1979). *RAN Sea King Environment Survey Part 2: Measurement of Temperature and Humidity*. Mech. Eng. Note 377. Nov. 1979. Melbourne: Aeronautical Research Laboratories.

ACKNOWLEDGEMENT

Mr B. Humphreys of Marlandaire Pty. Ltd. provided advice and the loan of components when problems were encountered with development of the system.

APPENDIX 1

Test Results for Cooling System with Single Imperial 5 Evaporator Assembly

Test Number:	1	2
Compressor:		
Speed (r/min)	2713	2713
Power (kW)	2.47	2.57
Condenser:		
Air mass flow (kg/s)	0.680	0.703
Air inlet temp. (°C)	34.5	20.5
Refrigerant inlet temp. (°C)	94	80
Refrigerant outlet temp. (°C)	48.5	32.5
Refrigerant pressure (kPa abs.)	1306	881
(lbf/in ² gauge)	175	113
Refrigerant subcooling at outlet (°C)	4.8	4.1
Evaporator:		
Inlet air temp. (°C)	34.0	21.6
Outlet air temp. (°C)	10.6	2.3
Fan motor voltage (V)	14.0	15.0
Air mass flow (kg/s)	0.139	0.148
Condensate collection rate (kg/h)	0.80	1.20
Cooling effect—Sensible (kW)	3.25	2.85
Latent (kW)	0.55	0.82
Total (kW)	3.80	3.67
Refrigerant outlet temp. (°C)	6.0	-2.7
Refrigerant outlet pressure (kPa abs.)	256	208
(lbf/in ² gauge)	22.5	15.5
Refrigerant superheat at outlet (°C)	11.6	8.4
Compressor pressure ratio	5.10	4.23
Coefficient of performance	1.54	1.43

APPENDIX 2

Test Results for Cooling System with Two Parallel Imperial 5 Evaporator Assemblies

Test Number:	3	4	5
Compressor:			
Speed (r/min)	2713	2713	2713
Power (kW)	2.46	2.46	3.24
Condenser:			
Air mass flow (kg/s)	0.537	0.667	0.673
Air inlet temp. (°C)	21.6	22.5	33.8
Refrigerant inlet temp. (°C)	80.0	80.0	92.5
Refrigerant outlet temp. (°C)	38.5	39.0	56.5
Refrigerant pressure (kPa abs.)	1081	1102	1480
(lbf/in ² gauge)	142	145	200
Refrigerant subcooling at outlet (°C)	6	6.5	2.4
Evaporator:			
Inlet air temp. (°C)	23.0	24.5	34.6
Outlet air temp. (°C)	7.8	9.8	15.5
Fan motor voltage (V)	12.3	14.0	14.07
Air mass flow (kg/s)	0.248	0.278	0.280
Condensate collection rate (kg/h)	2.00	2.04	0.0
Cooling effect—Sensible (kW)	3.76	4.09	5.35
Latent (kW)	1.36	1.39	0.0
Total (kW)	5.12	5.48	5.33
Refrigerant outlet temp. (°C)	3.0	5.0	12.0
Refrigerant outlet pressure (kPa abs.)	273	297	345
(lbf/in ² gauge)	25.0	28.5	35.4
Refrigerant superheat at outlet (°C)	6.3	6.1	8.7
Compressor pressure ratio	3.96	3.71	4.30
Coefficient of performance	2.04	2.21	1.64

APPENDIX 3

Cooling System Test Results (Tests 1-14)

Test Number:	1	2	3	4	5	6	7	8	9	10	11	12	13	14
Compressor:														
Speed (r/min)	2980	2980	2980	2980	2980	2980	2975	2980	2980	2000	2000	2000	2000	2000
Power (kW)	4.25	3.09	2.91	4.18	3.12	3.09	4.59	3.84	3.06	2.50	2.19	2.03	2.61	2.35
R12 inlet temp. (°C)	9.7	-6.9	-8.1	8.9	3.2	8.2	13.2	8.7	3.6	9.9	3.3	7.1	11.1	7.7
R12 inlet pressure (kPa abs.)	308	248	239	318	247	238	346	285	238	308	259	244	328	284
(lbf/in ² gauge)	30.0	21.3	20.0	31.5	21.2	19.9	35.5	26.7	19.9	30.0	23.0	20.8	33.0	26.5
R12 outlet temp. (°C)	94.2	75.7	—	98.9	102.2	82.1	107.3	109.3	—	83.8	80.2	72.6	87.9	92.2
R12 outlet pressure (kPa abs.)	1239	1191	1170	1529	1584	1522	1825	1791	1922	1239	1149	1136	1466	1494
(lbf/in ² gauge)	165	158	155	207	215	206	250	245	264	165	152	150	198	202
Pressure ratio	4.02	4.80	4.90	4.81	6.41	6.39	5.27	6.28	8.08	4.02	4.44	4.66	4.47	5.26
Condenser:														
Air mass flow (kg/s)	1.12	1.15	0.95	0.89	1.25	1.25	0.63	0.32	0.85	1.10	1.06	1.06	1.04	0.93
Air inlet temp. (°C)	29.1	20.9	26.1	36.0	31.9	35.8	39.0	36.0	41.1	21.8	21.9	22.9	26.0	30.0
R12 outlet temp. (°C)	42.0	21.6	25.8	49.1	29.8	32.4	54.7	53.2	37.1	22.9	23.4	23.6	27.8	30.7
R12 outlet pressure (kPa abs.)	1080	1066	1052	1397	1493	1431	1893	1707	1858	1135	1066	1038	1342	1424
(lbf/in ² gauge)	142	140	138	188	202	193	260	233	255	150	140	136	180	192
R12 subcooling at outlet (°C)	3.0	22.8	18.0	7.0	29.6	24.8	16.4	10.1	31.7	24.3	21.0	19.7	26.6	26.5
Evaporator:														
Inlet air temp. (°C)	30.7	27.9	28.7	31.0	27.7	28.5	33.0	30.4	28.8	28.2	28.7	28.5	29.4	28.9
Outlet air temp. (°C)	18.5	9.4	5.9	19.0	9.9	5.4	20.7	13.0	5.0	17.9	11.1	6.3	18.5	12.2
Air mass flow (kg/s)	0.585	0.306	0.188	0.576	0.306	0.181	0.574	0.302	0.181	0.598	0.302	0.192	0.598	0.302
Cooling effect (kW)	7.21	5.72	4.33	6.98	5.50	4.22	7.13	5.31	4.35	6.22	5.37	4.31	6.58	5.09
R12 inlet temp. (°C)	38.0	36.0	22.0	42.0	23.5	25.8	47.0	45.3	28.0	23.0	—	25.0	29.0	29.0
R12 outlet temp. (°C)	11.6	-2.1	-3.1	8.6	1.6	-3.2	15.1	8.6	3.4	10.2	1.3	-1.3	12.3	3.2
R12 outlet pressure (kPa abs.)	385	291	287	398	294	277	419	340	274	353	291	272	379	318
(lbf/in ² gauge)	41.2	27.5	27.0	43.0	28.0	25.5	46.1	34.6	25.0	36.5	27.5	24.8	40.3	31.4
R12 superheat at outlet (°C)	4.4	-0.4	-1.0	0.8	2.7	0	5.1	5.8	0	5.7	3.0	1.4	5.6	2.1
Coefficient of performance	1.70	1.85	1.49	1.67	1.76	1.37	1.55	1.38	1.42	2.49	2.45	2.12	2.52	2.17
Refrigerant mass flow (g/s)	65.5	55.1	53.1	64.7	47.0	—	68.4	55.2	43.2	51.7	44.0	43.1	53.2	44.3
Volumetric efficiency of compressor	0.54	0.54	0.53	0.52	0.48	—	0.51	0.49	0.46	0.64	0.63	0.63	0.62	0.58
Isentropic efficiency of compressor	0.71	0.78	—	0.75	0.78	0.86	0.79	0.74	—	0.82	0.80	0.78	0.86	0.84

Cooling System Test Results (Tests 15-27)

Test Number:	15	16	17	18	19	20	21	22	23	24	25	26	27
Compressor:													
Speed (r/min)	2000	2000	2000	2000	1000	1000	1000	1000	1000	1000	1000	1000	1000
Power (kW)	2.19	2.69	2.46	2.36	1.28	1.20	1.15	1.49	1.38	1.31	1.62	1.54	1.41
R12 inlet temp. (°C)	1.4	10.6	7.9	0.4	11.6	10.8	6.8	13.7	11.1	10.0	13.9	11.6	10.3
R12 inlet pressure (kPa abs.)	259	327	296	265	404	351	322	417	360	337	429	385	344
(lbf/in ² gauge)	23	32.8	28.2	23.8	44.0	36.2	32.0	45.8	37.5	34.2	47.5	41.2	35.2
R12 outlet temp. (°C)	89.1	99.4	100.9	96.7	64.4	66.4	65.8	75.9	79.4	81.1	85.1	86.7	90.4
R12 outlet pressure (kPa abs.)	1472	1789	1824	1769	1135	1135	1100	1493	1514	1548	1851	1824	1858
(lbf/in ² gauge)	199	245	250	242	150	150	145	202	205	210	254	250	255
Pressure ratio	5.7	5.5	6.2	6.7	2.8	3.2	3.4	3.6	4.2	4.6	4.3	4.7	5.4
Condenser:													
Air mass flow (kg/s)	0.88	0.82	0.93	0.80	0.85	0.81	0.73	0.93	0.80	0.70	0.82	0.76	0.52
Air inlet temp. (°C)	30.0	31.5	37.0	39.0	24.0	27.1	27.0	33.2	34.1	34.8	42.7	45.3	24.3
R12 outlet temp. (°C)	31.0	32.7	35.9	36.9	24.4	27.3	28.1	33.6	34.6	35.1	41.3	42.3	26.3
R12 outlet pressure (kPa abs.)	1410	1700	1755	1714	1080	1080	1066	1466	1479	1514	1824	1810	1824
(lbf/in ² gauge)	190	232	240	234	142	142	140	198	200	205	250	248	250
R12 subcooling at outlet (°C)	25.2	33.1	30.2	28.1	24.5	21.6	20.8	25.2	23.7	24.9	23.7	21.5	38.7
Evaporator:													
Inlet air temp. (°C)	29.0	27.3	29.3	29.5	31.0	30.4	29.8	30.0	28.5	29.2	29.5	30.1	28.9
Outlet air temp. (°C)	7.6	17.4	12.7	7.0	22.3	16.7	12.5	21.5	16.4	13.3	21.6	17.5	13.2
Air mass flow (kg/s)	0.201	0.595	0.314	0.185	0.598	0.304	0.208	0.585	0.310	0.208	0.580	0.306	0.204
Cooling effect (kW)	4.34	5.95	5.26	4.20	5.25	4.21	3.63	5.02	3.79	3.34	4.63	3.89	3.23
R12 inlet temp. (°C)	28.5	30.5	31.0	30.5	24.5	25.4	25.6	30.2	30.0	31.0	33.0	35.0	26.8
R12 outlet temp. (°C)	-0.7	10.6	5.8	-0.9	11.9	7.1	4.2	13.3	9.6	7.8	14.2	10.3	10.0
R12 outlet pressure (kPa abs.)	287	364	329	289	429	370	330	440	377	351	449	403	346
(lbf/in ² gauge)	27.0	38.2	33.0	27.3	47.5	39.0	33.2	49.2	40.0	36.2	50.4	43.8	35.5
R12 superheat at outlet (°C)	1.5	5.0	3.5	1.3	1.34	1.5	2.0	1.6	2.9	3.3	2.0	2.0	6.6
Coefficient of performance	1.98	2.21	2.14	1.78	4.1	3.51	3.16	3.37	2.75	2.55	2.86	2.53	2.29
Refrigerant mass flow (g/s)	40.5	50.0	44.1	39.4	44.3	37.1	31.5	42.3	34.3	—	—	—	—
Volumetric efficiency of compressor	0.58	0.58	0.56	0.56	0.83	0.80	0.75	0.78	0.73	—	—	—	—
Isentropic efficiency of compressor	0.85	0.82	0.85	0.84	0.83	0.89	0.81	0.93	0.95	0.94	0.92	0.92	0.91

APPENDIX 4

Test Results with Varying Evaporator Inlet Air Temperature

Test Number:	28	29	30	31	32
Compressor:					
Type	York 209	York 209	York 209	York 209	York 209
Speed (r/min)	2000	2000	2000	2000	2000
Power (kW)	3.12	2.87	2.76	2.56	2.42
R12 inlet temp. (°C)	13.3	9.8	7.7	6.0	5.2
R12 inlet pressure (kPa abs.)	382	342	318	287	270
(lbf/in ² gauge)	40.8	35.0	31.5	27	24.5
R12 outlet temp. (°C)	91.6	93.3	94.1	95.5	97.1
R12 outlet pressure (kPa abs.)	1734	1741	1706	1713	1699
(lbf/in ² gauge)	237	238	233	234	232
Pressure ratio	4.54	5.09	5.37	5.97	6.30
Condenser:					
Air mass flow (kg/s)	1.09	1.09	1.08	1.00	1.02
Air inlet temp. (°C)	25.7	25.8	26.2	26.1	26.7
R12 outlet temp. (°C)	26.1	26.1	25.8	25.8	26.1
R12 outlet pressure (kPa abs.)	1610	1630	1623	1617	1637
(lbf/in ² gauge)	219	222	221	220	223
R12 subcooling at outlet (°C)	37.0	37.0	37.0	37.0	36.7
Evaporator:					
Inlet air temp (°C)	35.9	29.3	24.8	19.8	16.2
Outlet air temp (°C)	23.4	19.0	15.3	11.6	9.2
Air mass flow (kg/s)	0.582	0.589	0.593	0.598	0.602
Cooling effect (kW)	7.34	6.13	5.69	4.95	4.26
R12 inlet temp. (°C)	29.5	27.0	25.0	24.0	32.5
R12 outlet temp. (°C)	14.4	10.6	7.9	4.7	3.8
R12 outlet pressure (kPa abs.)	420	384	360	322	305
(lbf/in ² gauge)	46.2	41.0	37.5	32.0	29.5
R12 superheat at outlet (°C)	4.4	3.9	2.9	3.6	4.4
Coefficient of performance	2.35	2.13	2.06	1.93	1.76
Refrigerant mass flow (g/s)	62.1	51.4	49.2	43.7	39.0
Volumetric efficiency of compressor	0.63	0.57	0.59	0.57	0.53
Isentropic efficiency of compressor	0.87	0.85	0.86	0.84	0.84

APPENDIX 5

Data Points for Compressor Performance Characteristics

Test Number:	1	2	3	4	5	6	7	8	9	10	11	12	13	14
Condensing temp. (°C)	51.1	48.8	48.8	60.0	61.7	60.0	68.3	67.7	71.1	51.1	47.8	47.2	58.3	58.8
Saturation temp. (°C)	0.0	6.6	-7.7	1.1	-6.7	-7.7	3.3	-2.2	-7.7	0.0	4.4	-7.2	2.2	-2.2
Measured cooling capacity (kW)	7.21	5.72	4.33	6.98	5.5	4.22	7.13	5.31	4.35	6.22	5.37	4.31	6.58	5.09
Correction for 6°C subcooling (kW)	0.0	0.90	0.62	0.0	0.99	0.63	0.66	0.22	3.06	0.90	0.63	0.57	1.05	1.04
Cooling capacity for 6°C subcooling (kW)	7.21	4.82	3.71	6.98	4.51	3.59	6.47	5.09	3.29	5.32	4.74	3.74	5.53	4.05
Calculated condenser heat rejection* (kW)	10.56	7.00	5.91	10.14	7.25	5.27	10.27	7.89	6.09	7.72	6.89	5.44	8.11	6.43

Test Number:	15	16	17	18	19	20	21	22	23	24	25	26	27
Condensing temp. (°C)	58.3	67.2	68.3	67.2	47.2	47.2	45.5	58.8	60.0	60.5	69.4	68.3	69.4
Saturation temp. (°C)	-5.0	1.7	-1.1	-4.4	8.8	3.8	1.7	9.4	5.0	2.8	10.5	7.2	3.3
Measured cooling capacity (kW)	4.34	5.95	5.26	4.20	5.25	4.21	3.63	5.02	3.79	3.34	4.63	3.89	3.23
Correction for 6°C subcooling (kW)	0.74	1.30	1.02	0.83	0.78	0.56	0.45	0.79	1.04	0.53	0.76	0.57	0.85
Cooling capacity for 6°C subcooling (kW)	3.6	4.65	4.24	3.37	4.46	3.65	3.18	4.23	2.75	2.81	3.87	3.32	2.38
Calculated condenser heat rejection* (kW)	5.58	7.32	6.60	5.48	6.01	4.94	4.13	5.60	3.87	3.72	5.24	4.43	3.29

* The calculated condenser heat rejection is found from the sum of the cooling capacity for 6°C subcooling, and the power input to the refrigerant in the compression phase, the latter being found by multiplying the refrigerant mass flow by the change in enthalpy per kg refrigerant during the compression phase.

APPENDIX 6

Data Points for Extension of Evaporator Performance Characteristics

Test Number:	33	34	35	36	37	38	39
Inlet air temp. (°C)	38.0	29.3	22.5	21.2	37.0	37.5	21.5
Outlet air temp. (°C)	29.3	22.5	17.2	10.0	19.5	24.0	13.0
Air mass flow (kg/s)	0.550	0.570	0.580	0.209	0.209	0.273	0.280
Cooling Capacity (kW)	4.80	3.88	3.06	2.34	3.66	3.69	2.38
Refrigerant in (°C)	26.0	25.0	24.0	23.0	26.5	27.5	25.0
Refrigerant out (°C)	17.4	12.2	7.9	0.6	10.1	13.1	3.3
Refrigerant pressure (lbf/in ² gauge)	62.0	50.0	41.0	29.8	43.2	52.2	33.0
(kPa abs.)	528	445	383	306	398	460	328
Superheat (°C)	0.0	0.0	1.2	0.6	1.8	0.3	1.1
Saturation temp. (°C)	17.8	12.2	6.7	0.0	8.3	12.8	2.2

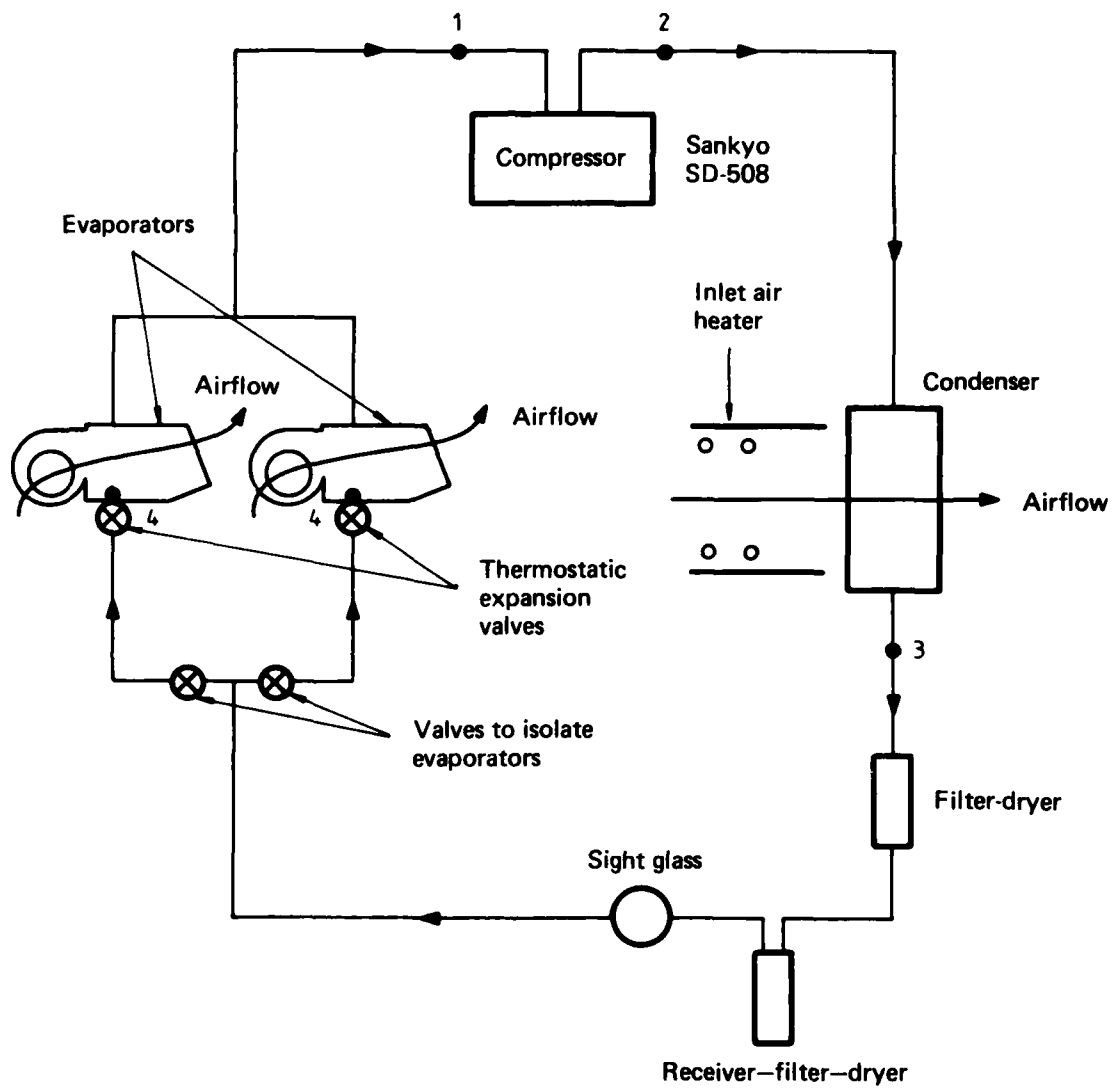


FIG. 1 SCHEMATIC DIAGRAM OF COOLING SYSTEM

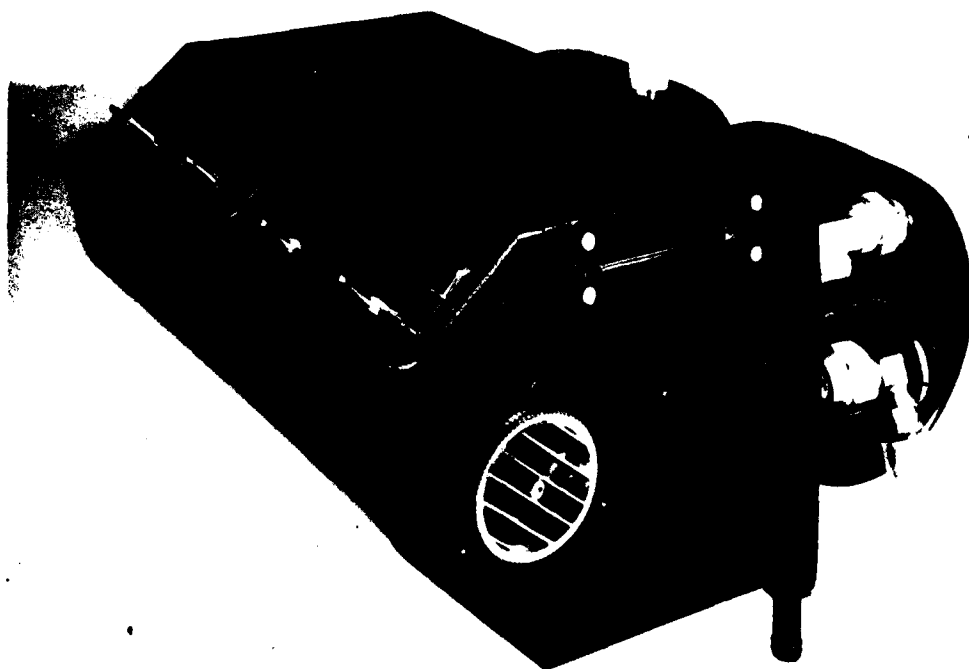


FIG. 2 COMPLETE UNICLA IMPERIAL 5 EVAPORATOR ASSEMBLY

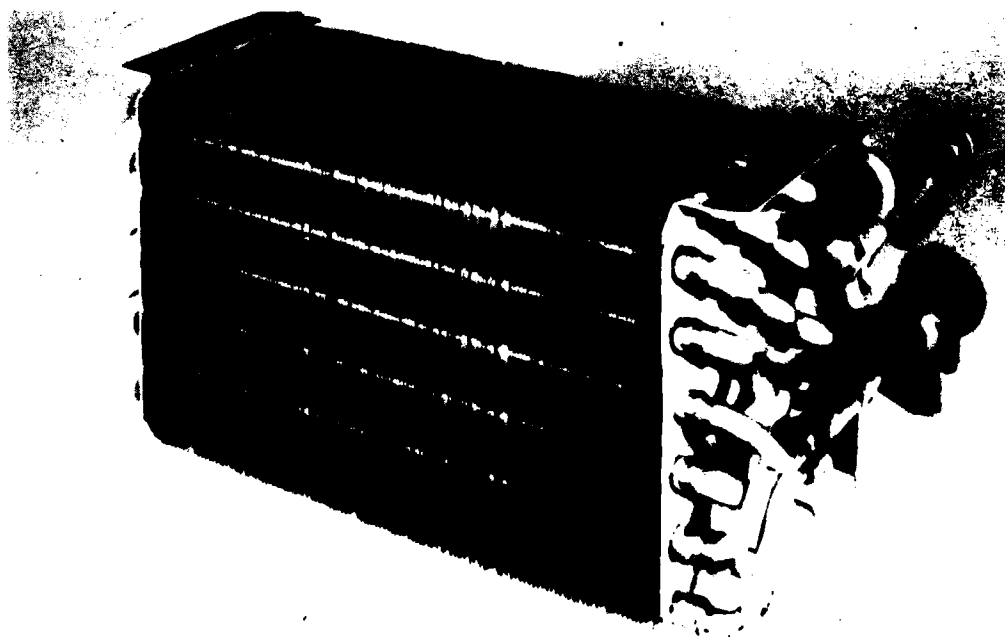


FIG. 3 EVAPORATOR MATRIX FROM IMPERIAL 5 EVAPORATOR ASSEMBLY

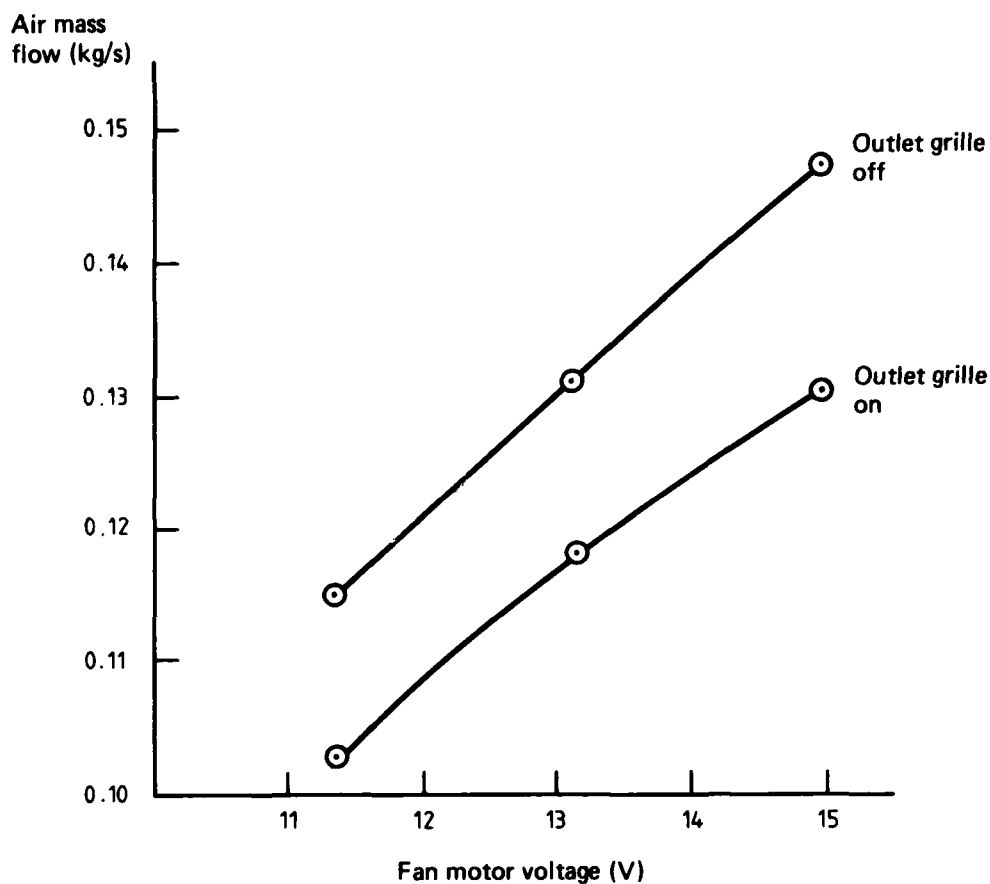
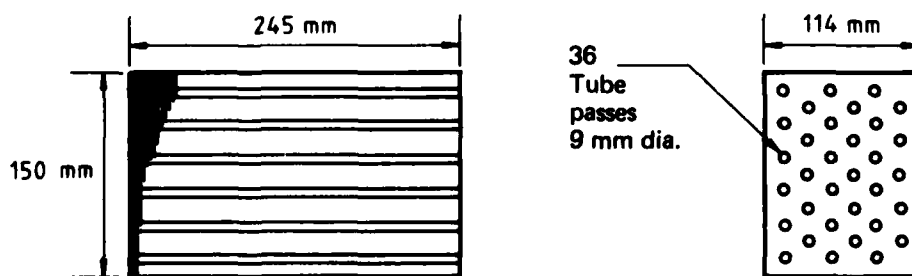


FIG. 4 AIRFLOW CALIBRATION FOR UNICLA IMPERIAL 5 EVAPORATOR-FAN ASSEMBLY



Weight: 2.05 kg (incl. T-X valve)

FIG. 5 EVAPORATOR MATRIX FROM IMPERIAL 5 EVAPORATOR ASSEMBLY

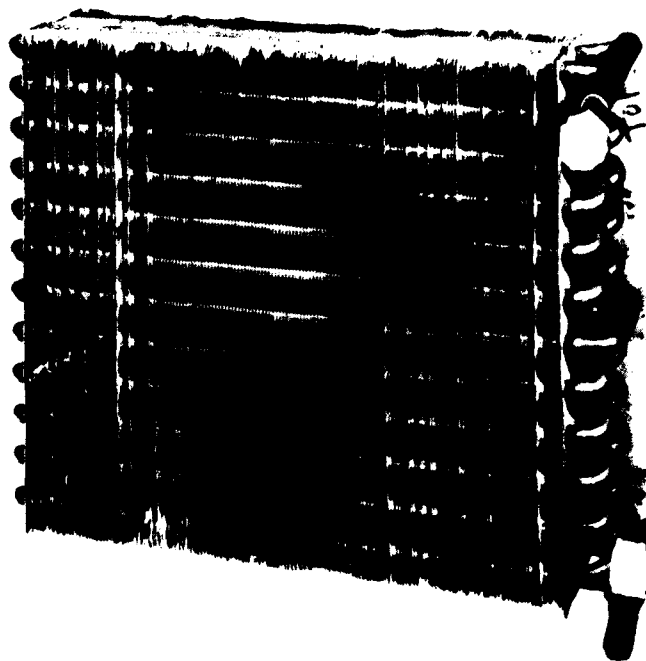
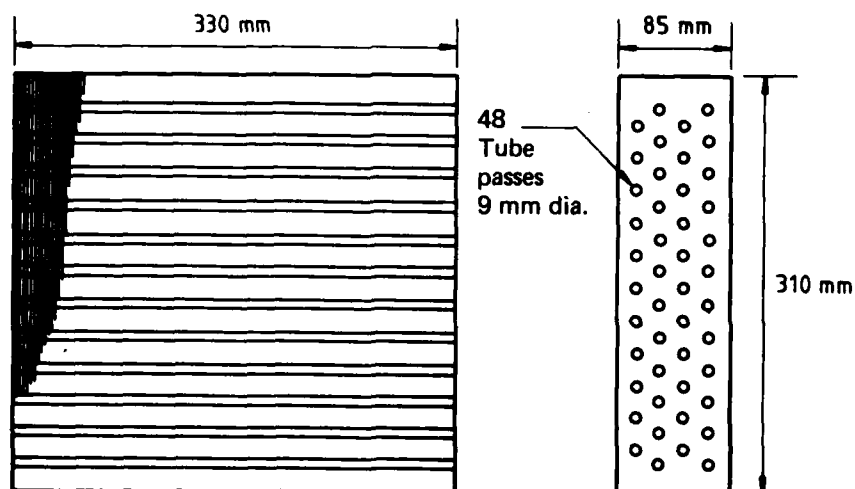
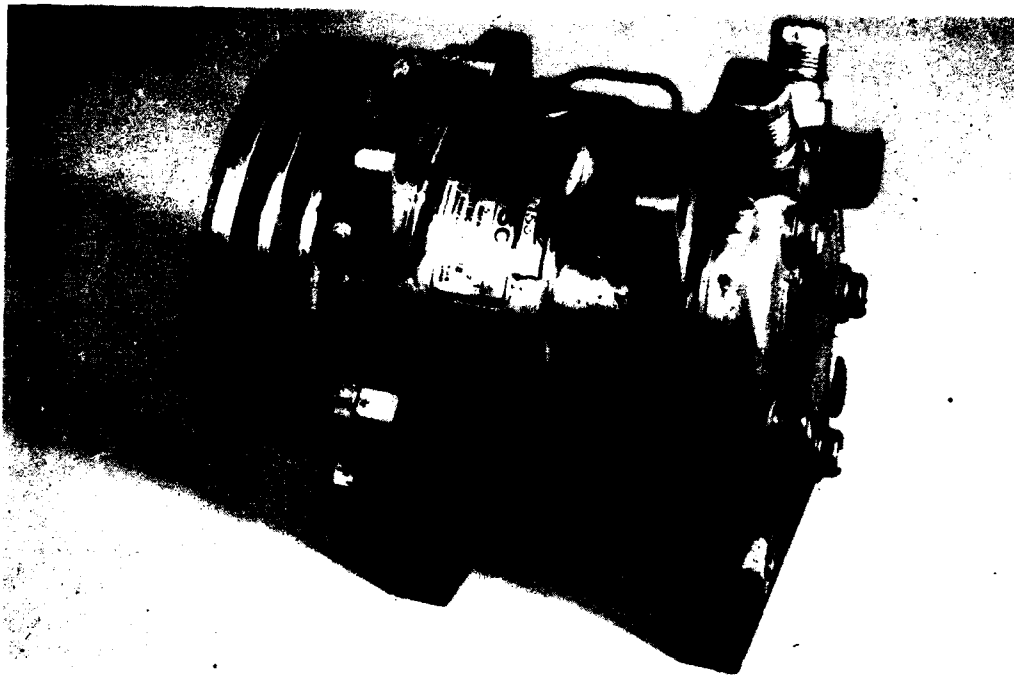


FIG. 6(a) CONDENSER USED FOR INITIAL TESTS



Weight: 4.10 kg

FIG. 6(b) CONDENSER DIMENSIONS AND TUBE CONFIGURATION



Overall length (including clutch) : 210 mm
Weight (with clutch) : 8.16 kg
Weight (without clutch) : 5.60 kg

FIG. 7 SANKYO SD 508 COMPRESSOR

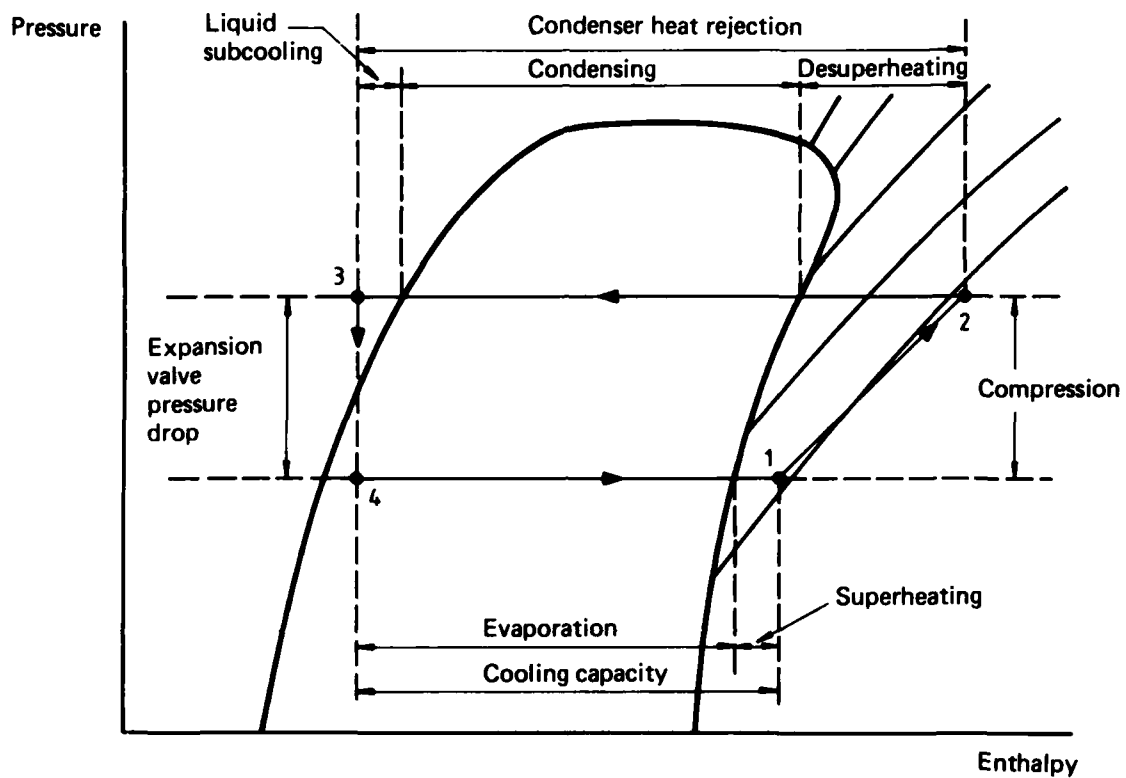


FIG. 8 TYPICAL PRESSURE-ENTHALPY DIAGRAM FOR A VAPOUR-CYCLE COOLING SYSTEM

(Points 1-4 shown on the schematic diagram of Fig. 1)

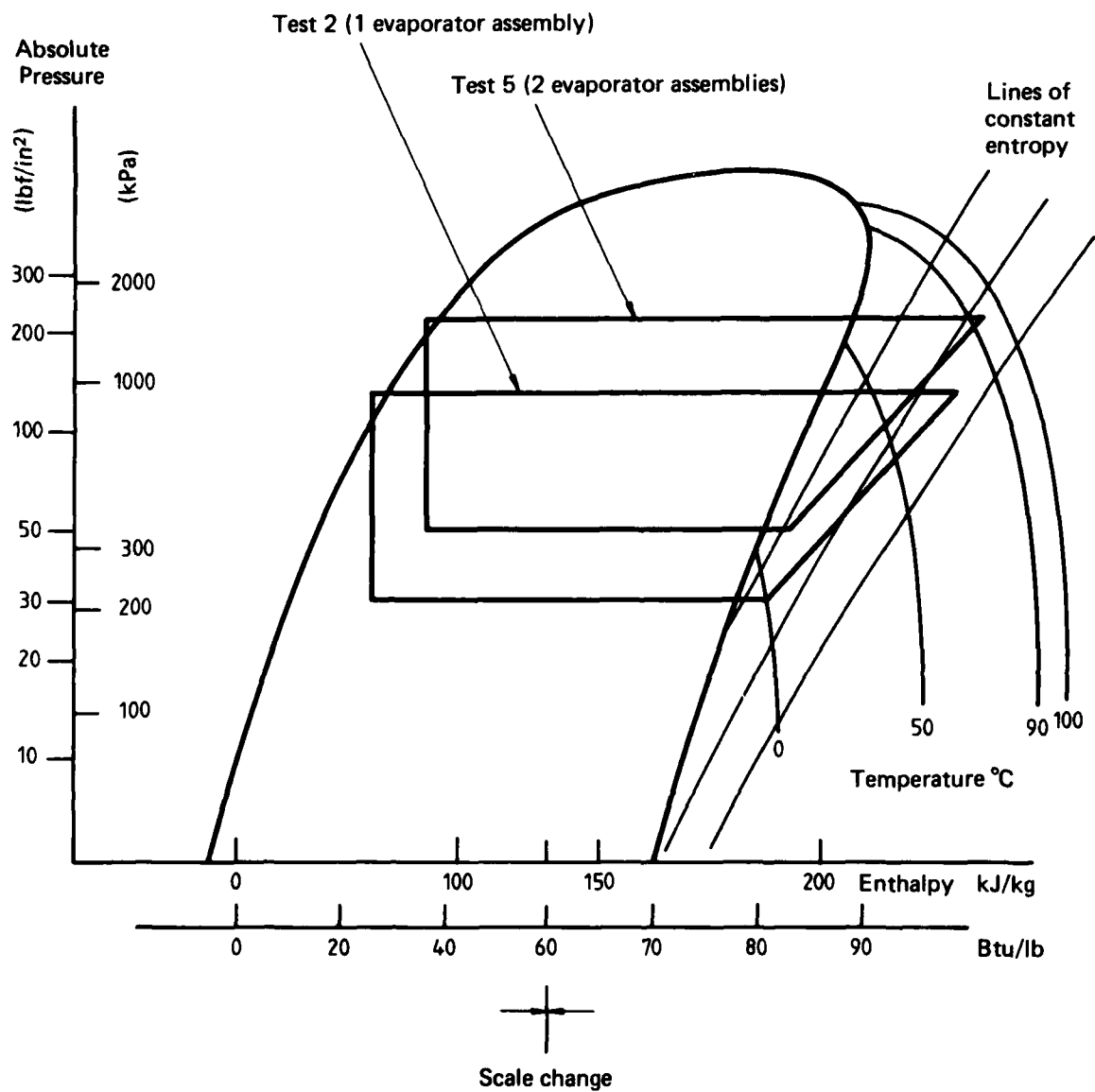


FIG. 9 PRESSURE-ENTHALPY DIAGRAM FOR TESTS 2 AND 5

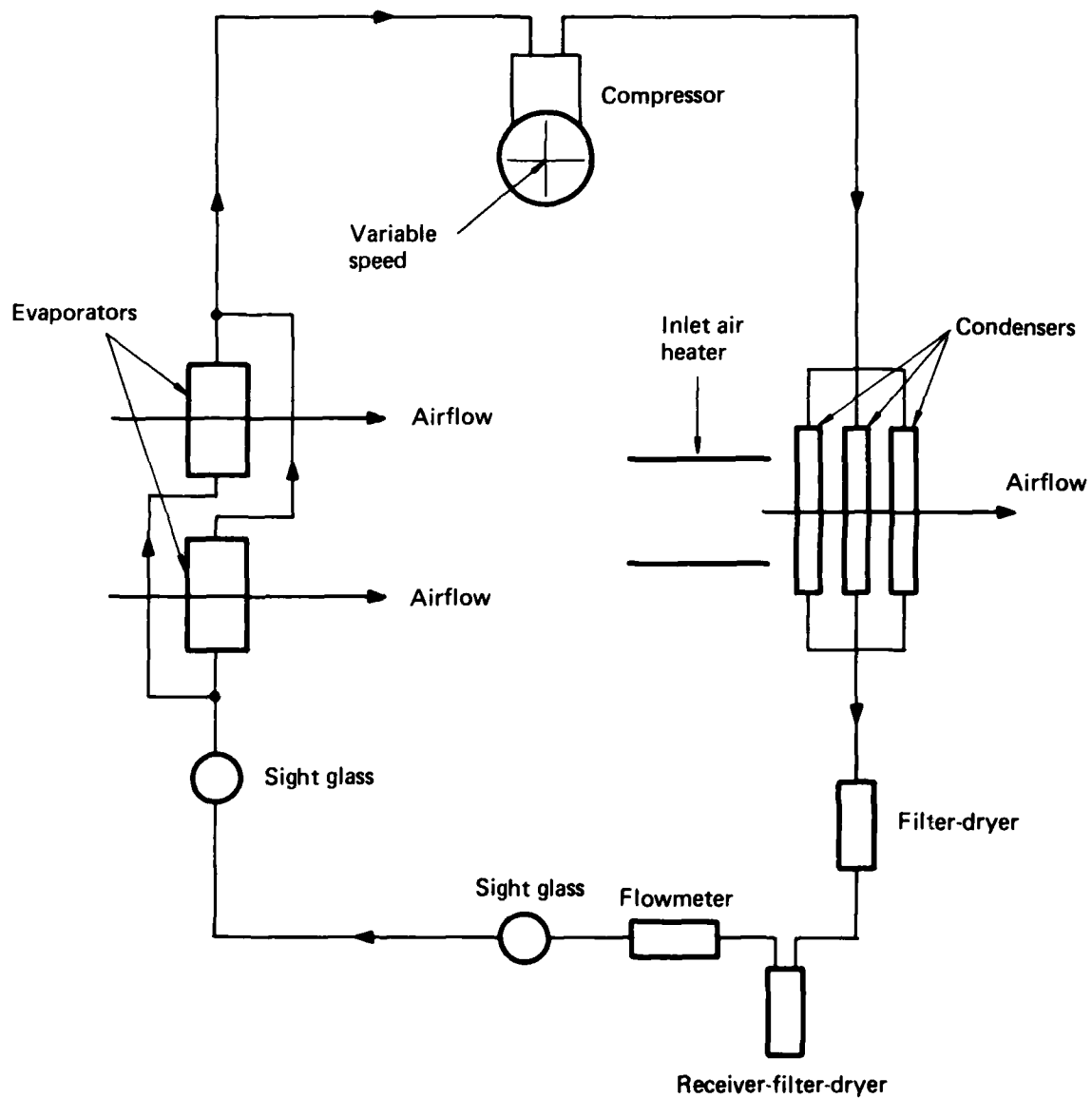


FIG. 10 SCHEMATIC DIAGRAM OF COOLING SYSTEM



FIG. 11 OVERALL LAYOUT

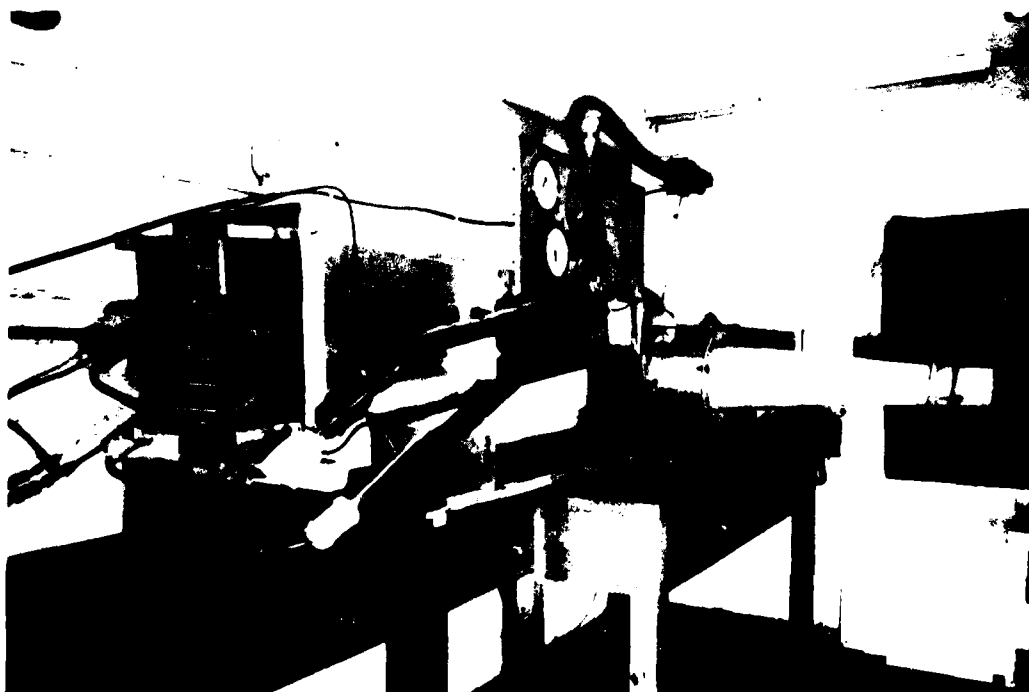
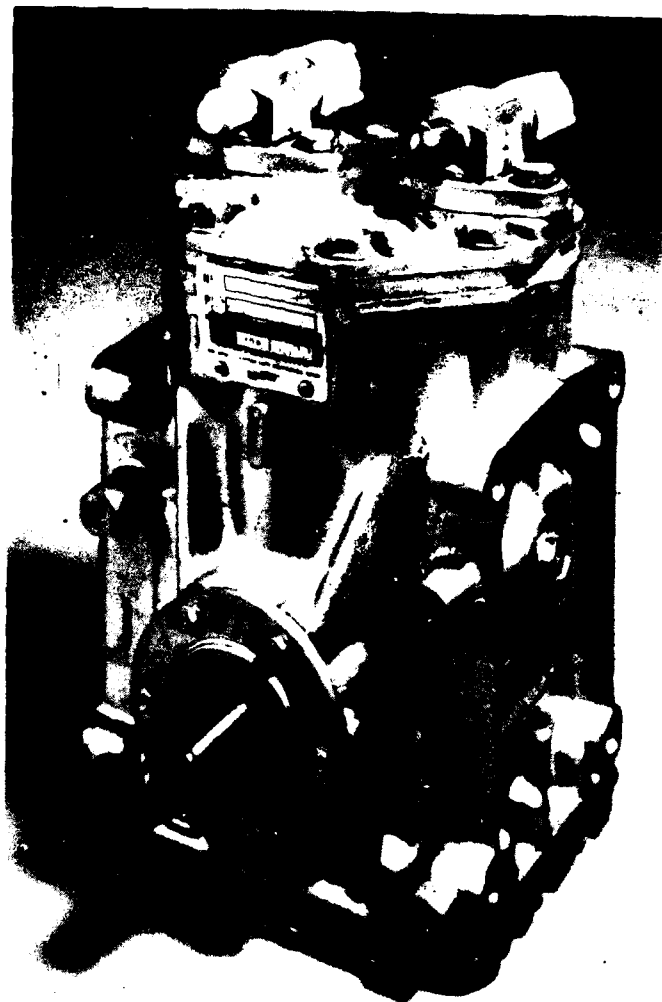


FIG. 12 EVAPORATOR TEST ROOM



Overall height	: 240 mm
width	: 140 mm
length (without clutch)	: 170 mm
Weight (with clutch)	: 9.88 kg
(without clutch)	: 6.62 kg

FIG. 13 YORK 209 REFRIGERANT COMPRESSOR

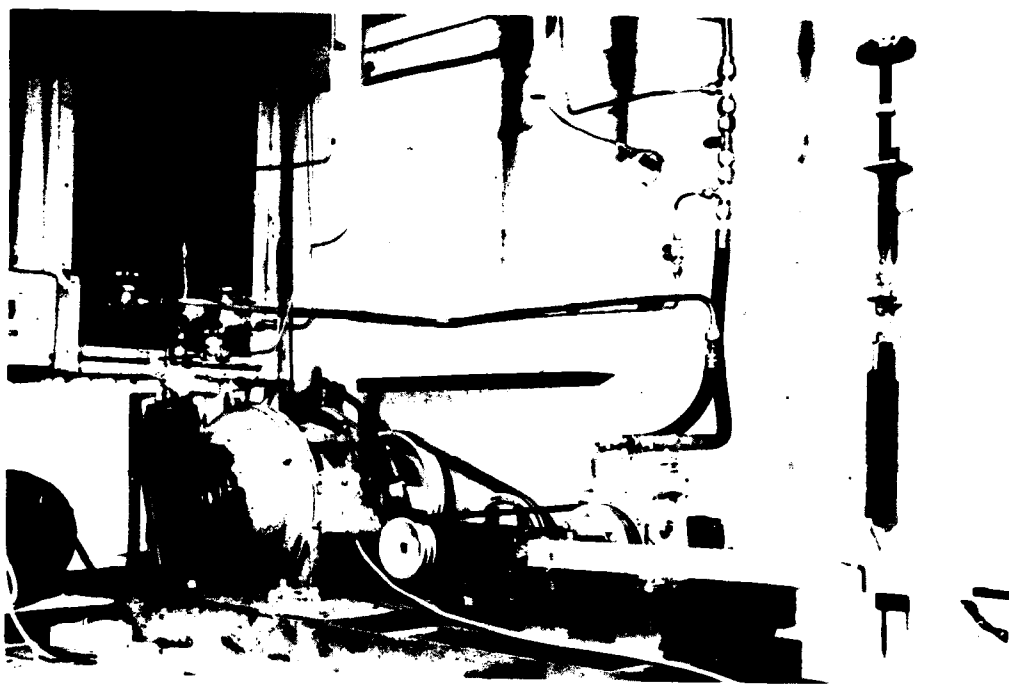


FIG. 14 COMPRESSOR INSTALLATION

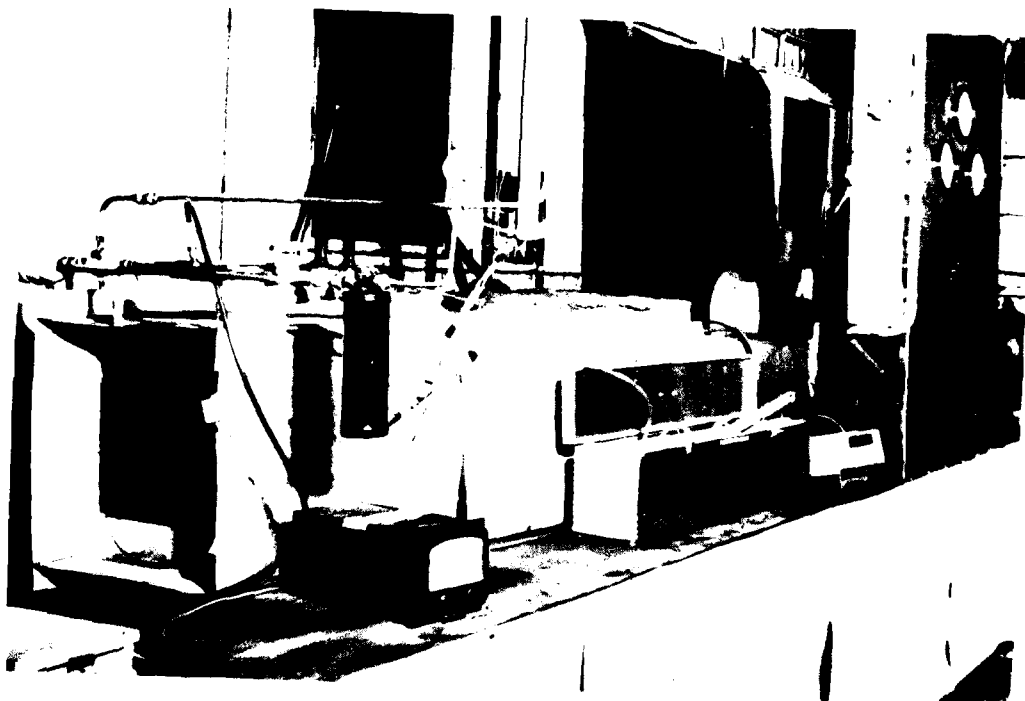


FIG. 15 CONDENSER INSTALLATION

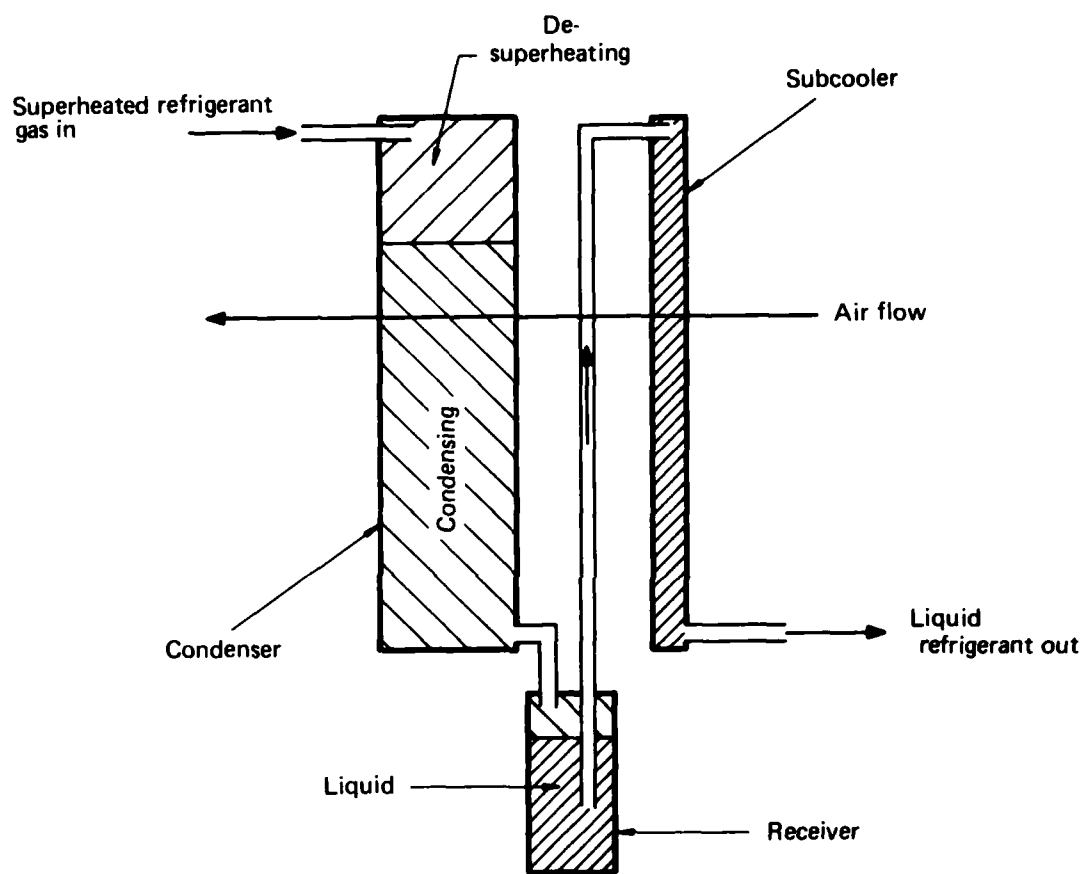
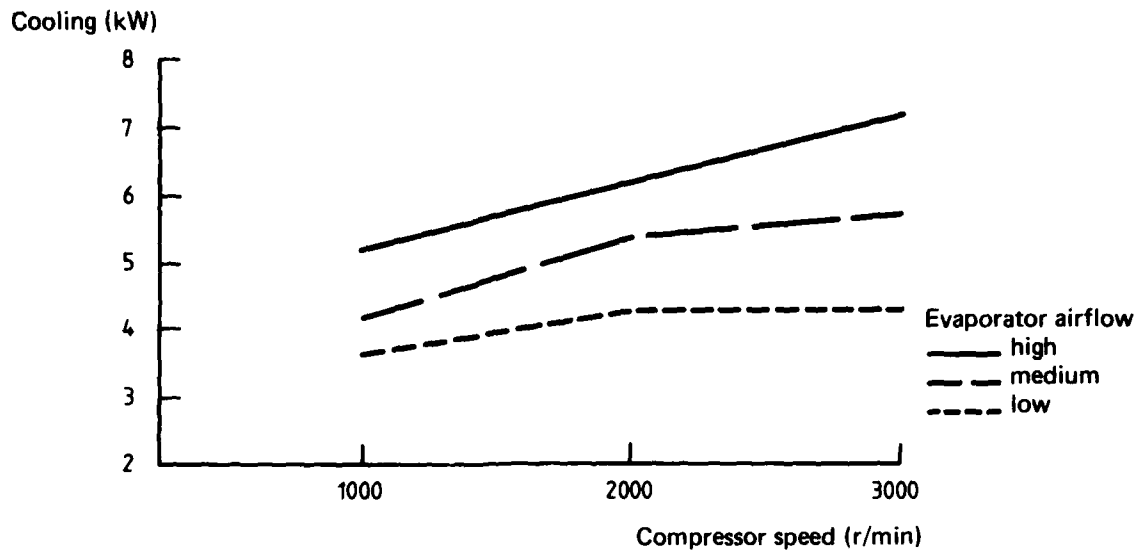
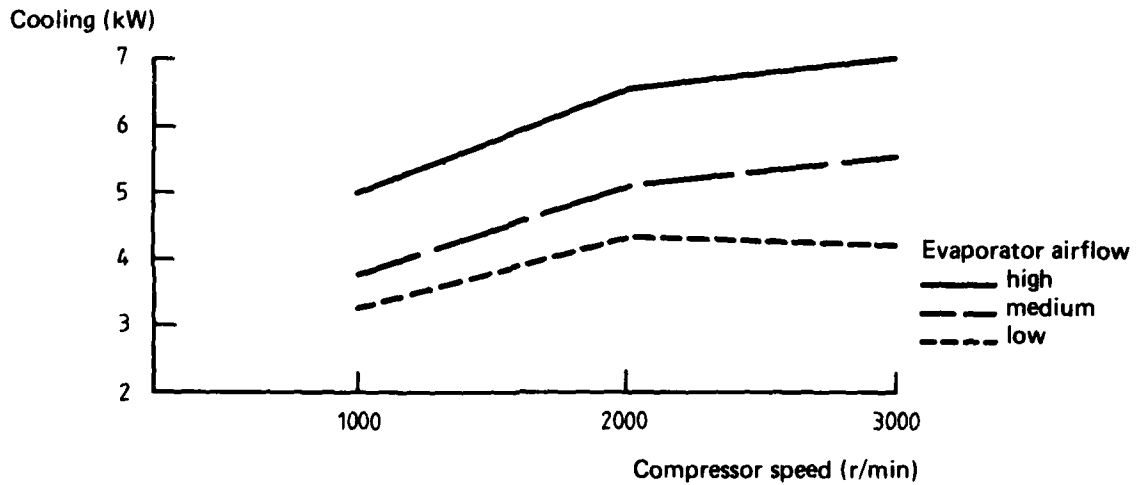


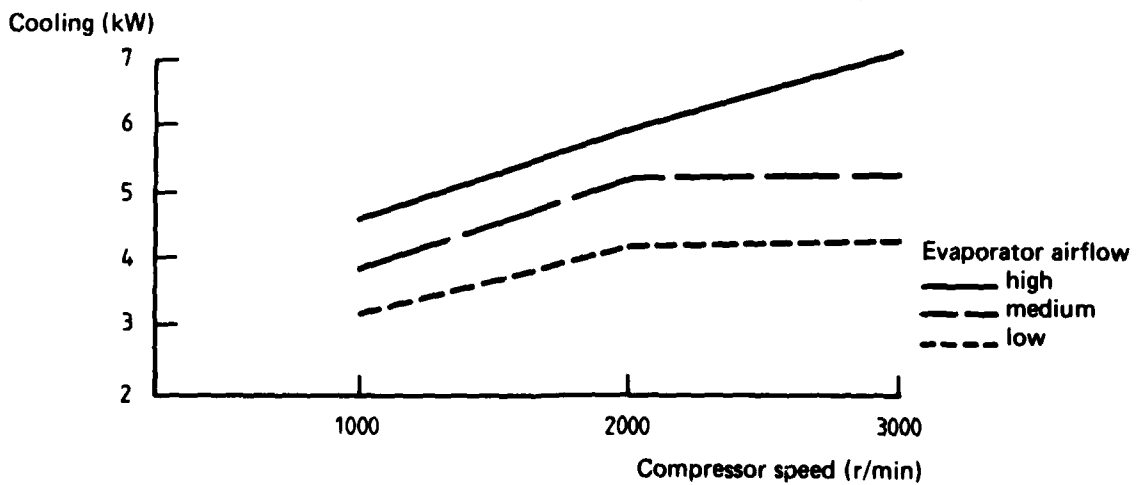
FIG. 16 CONDENSER OPERATION



(a) Compressor discharge pressure 1030 kPa (150 lbf/in²) gauge

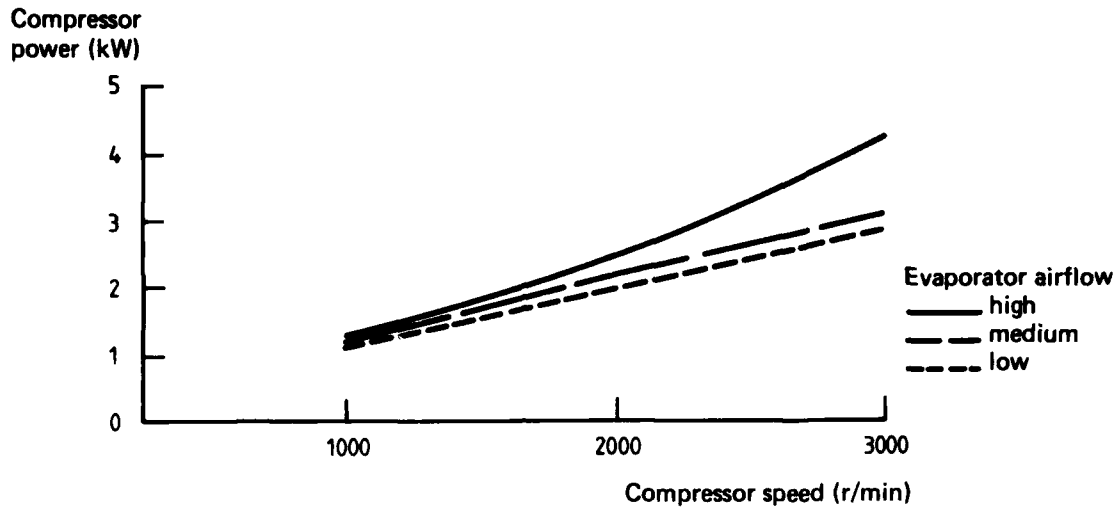


(b) Compressor discharge pressure 1380 kPa (200 lbf/in²) gauge

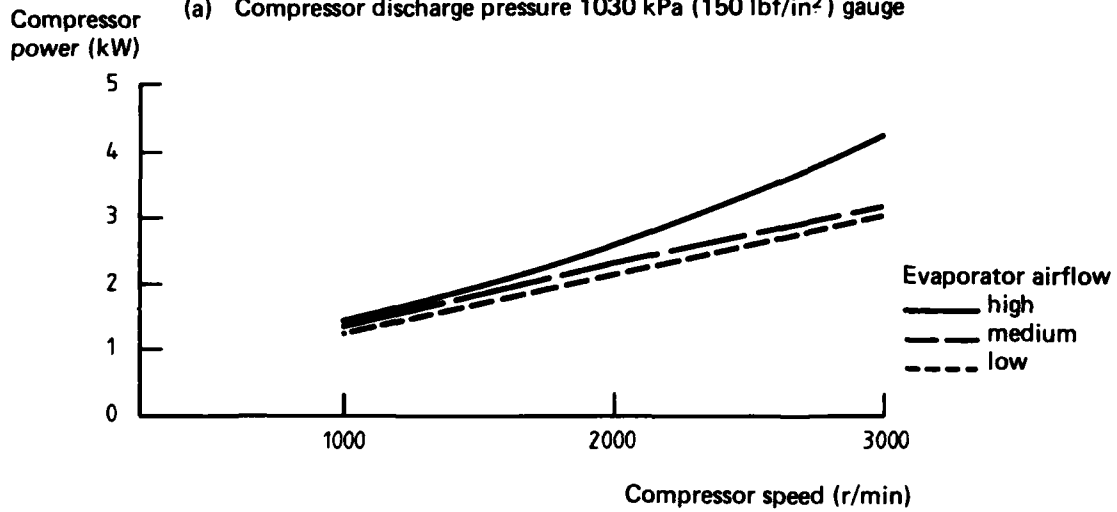


(c) Compressor discharge pressure 1720 kPa (250 lbf/in²) gauge

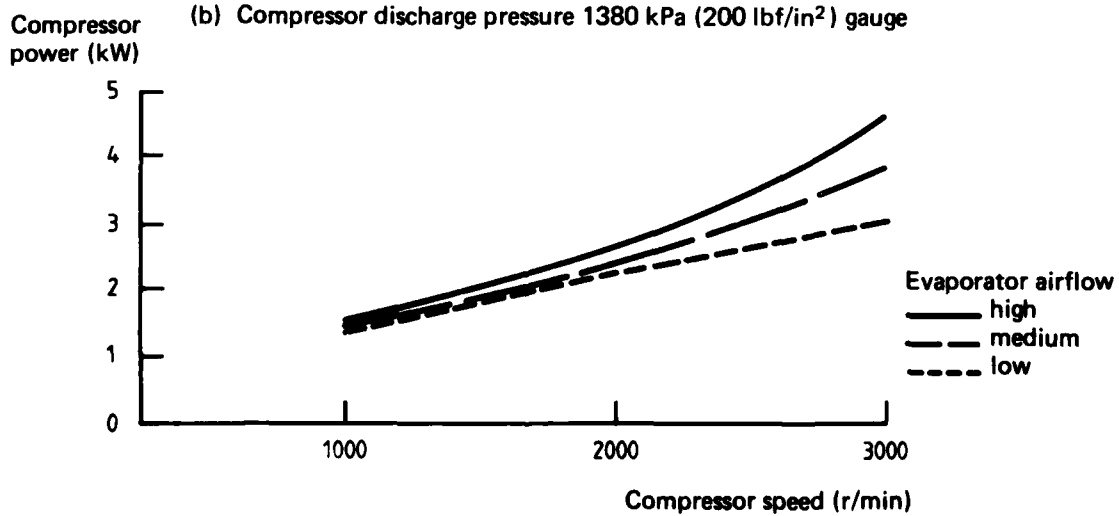
FIGS. 17a, b, c COOLING CAPACITY VS. COMPRESSOR SPEED (YORK 209 COMPRESSOR)



(a) Compressor discharge pressure 1030 kPa (150 lbf/in²) gauge

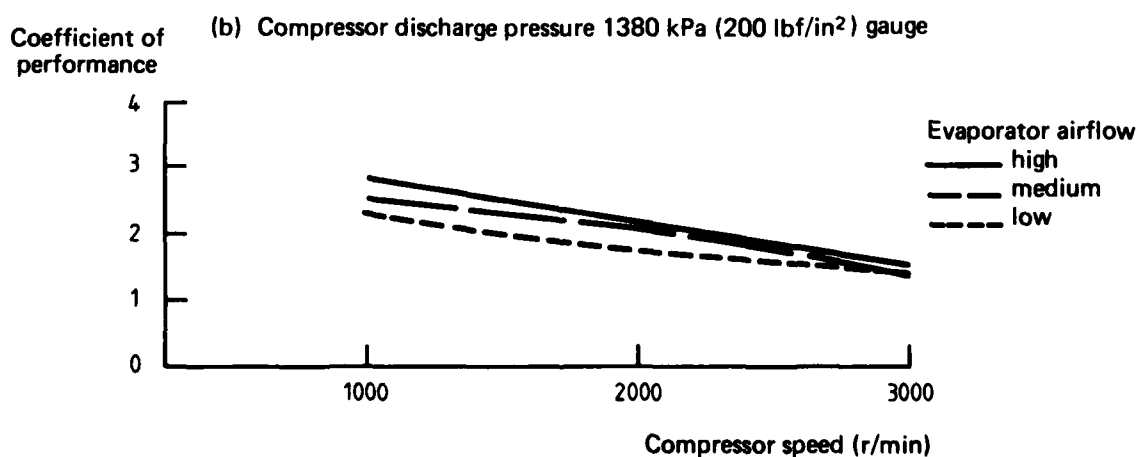
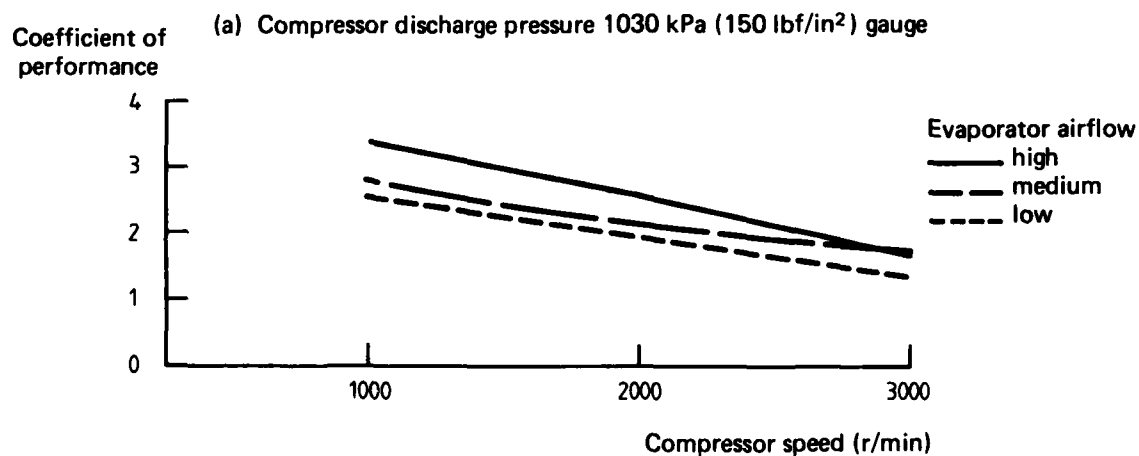
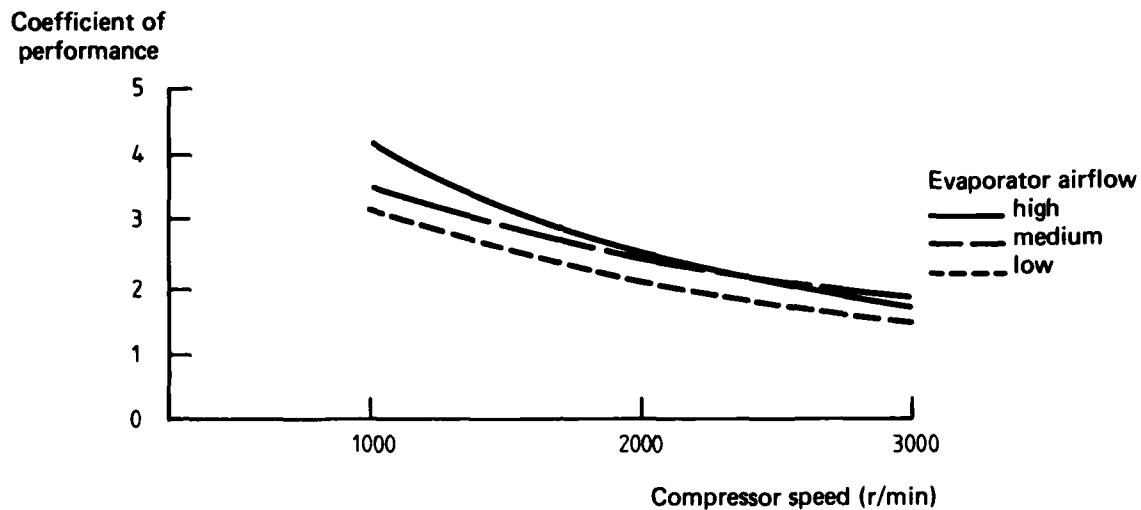


(b) Compressor discharge pressure 1380 kPa (200 lbf/in²) gauge



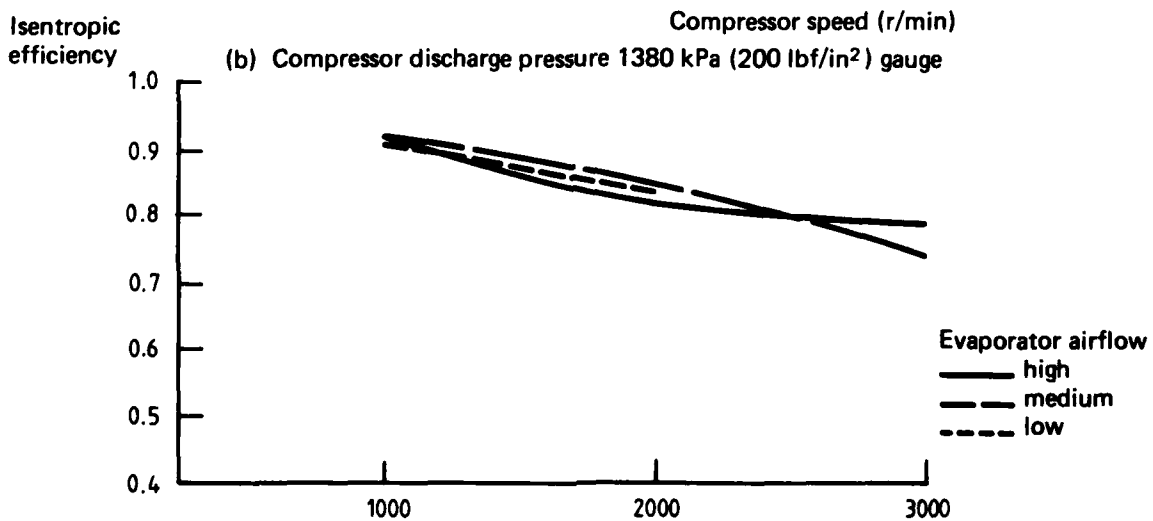
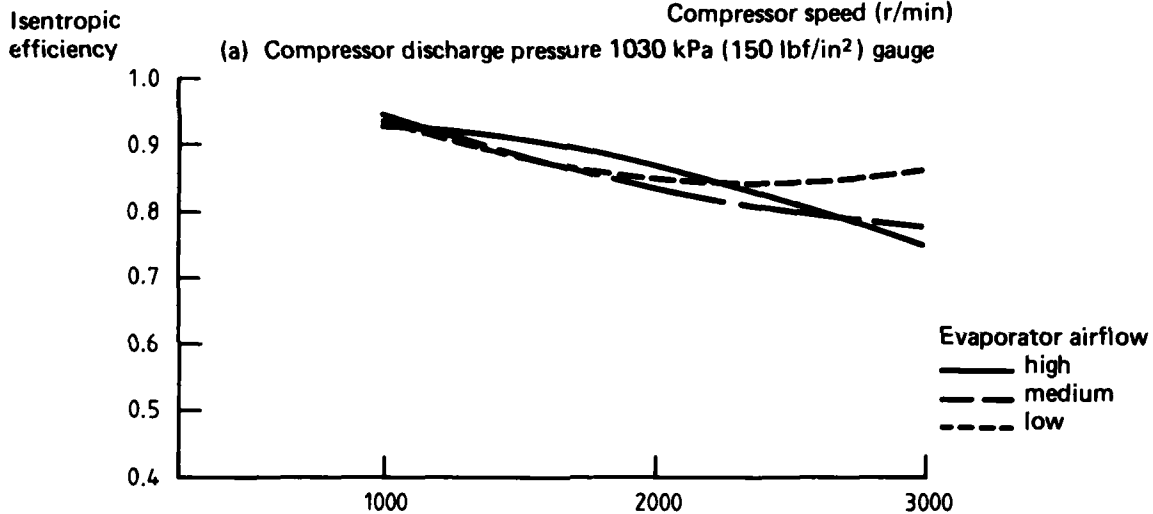
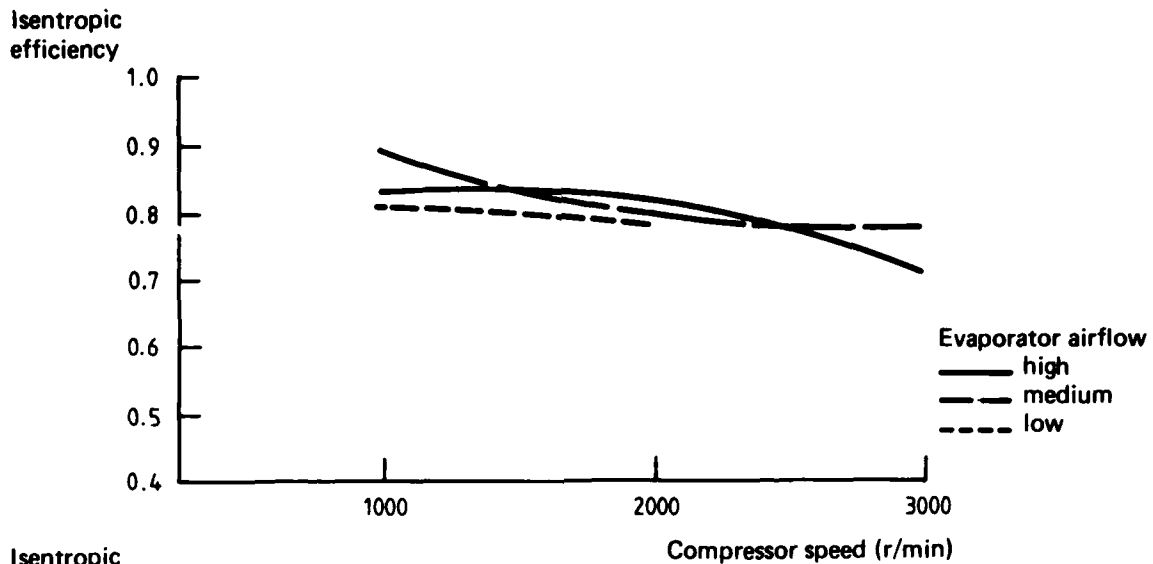
(c) Compressor discharge pressure 1720 kPa (250 lbf/in²) gauge

FIGS. 18a, b, c COMPRESSOR POWER CONSUMPTION VS. COMPRESSOR SPEED
(YORK 209 COMPRESSOR)

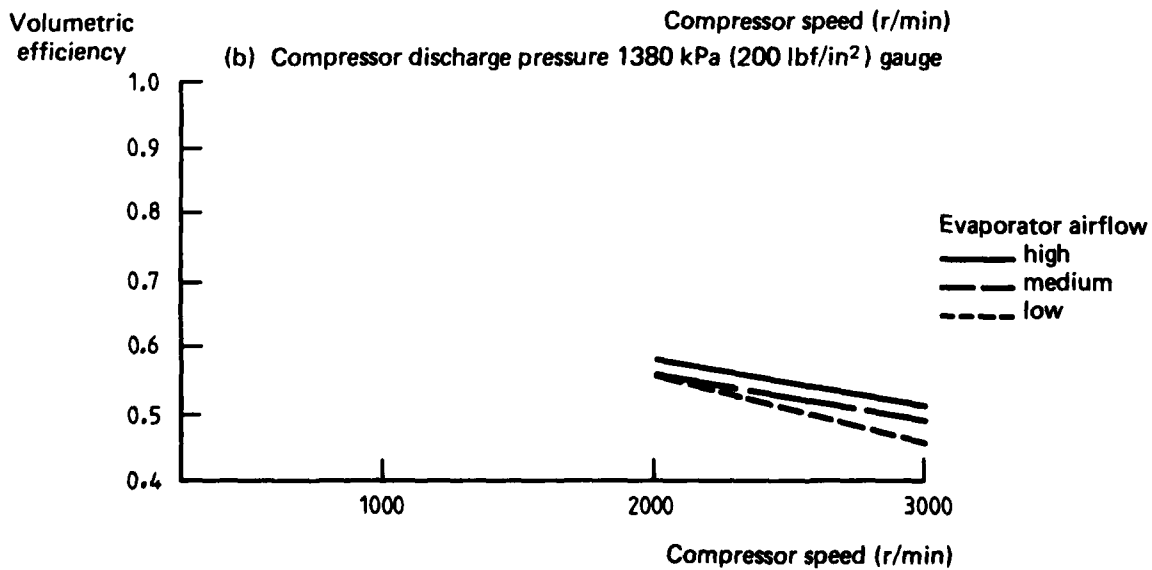
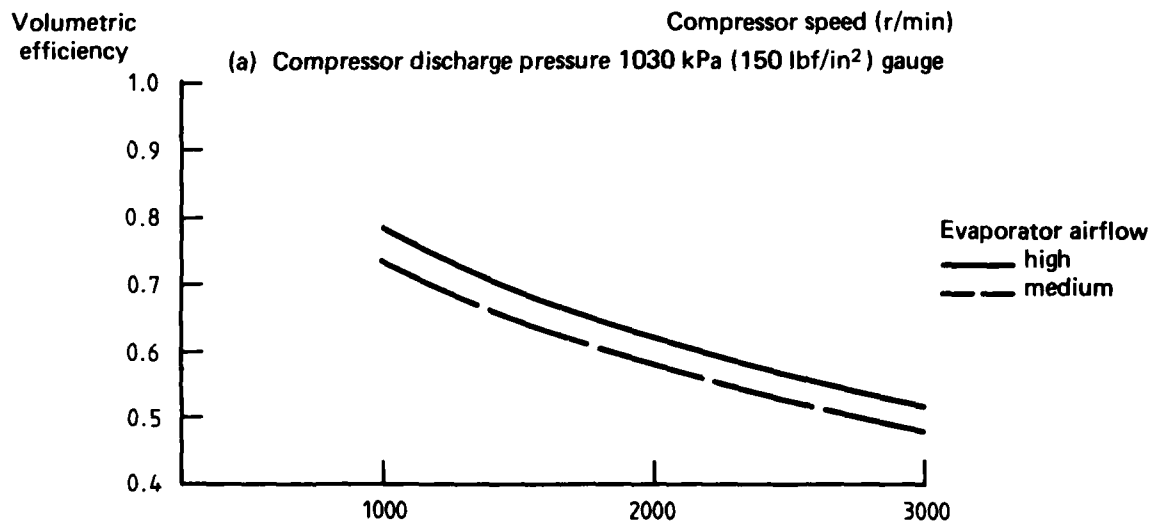
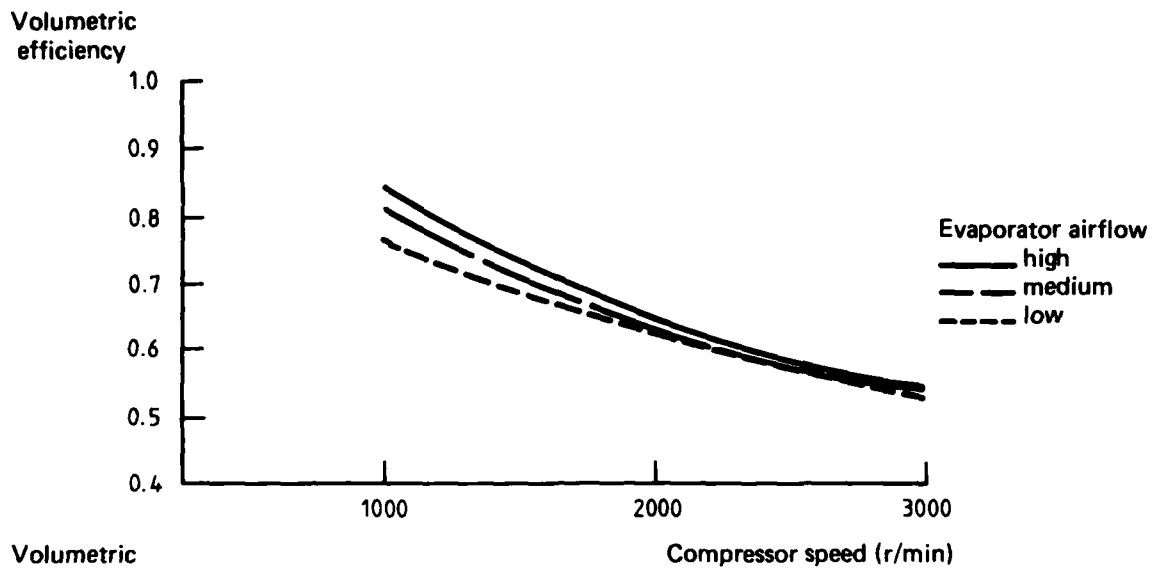


(c) Compressor discharge pressure 1720 kPa (250 lbf/in²) gauge

FIGS. 19a, b, c COEFFICIENT OF PERFORMANCE OF THE COOLING SYSTEM



FIGS 20a, b, c COMPRESSOR ISENTROPIC EFFICIENCY (YORK 209 COMPRESSOR)



(c) Compressor discharge pressure 1720 kPa (250 lbf/in²) gauge

FIGS. 21a, b, c COMPRESSOR VOLUMETRIC EFFICIENCY (YORK 209 COMPRESSOR)

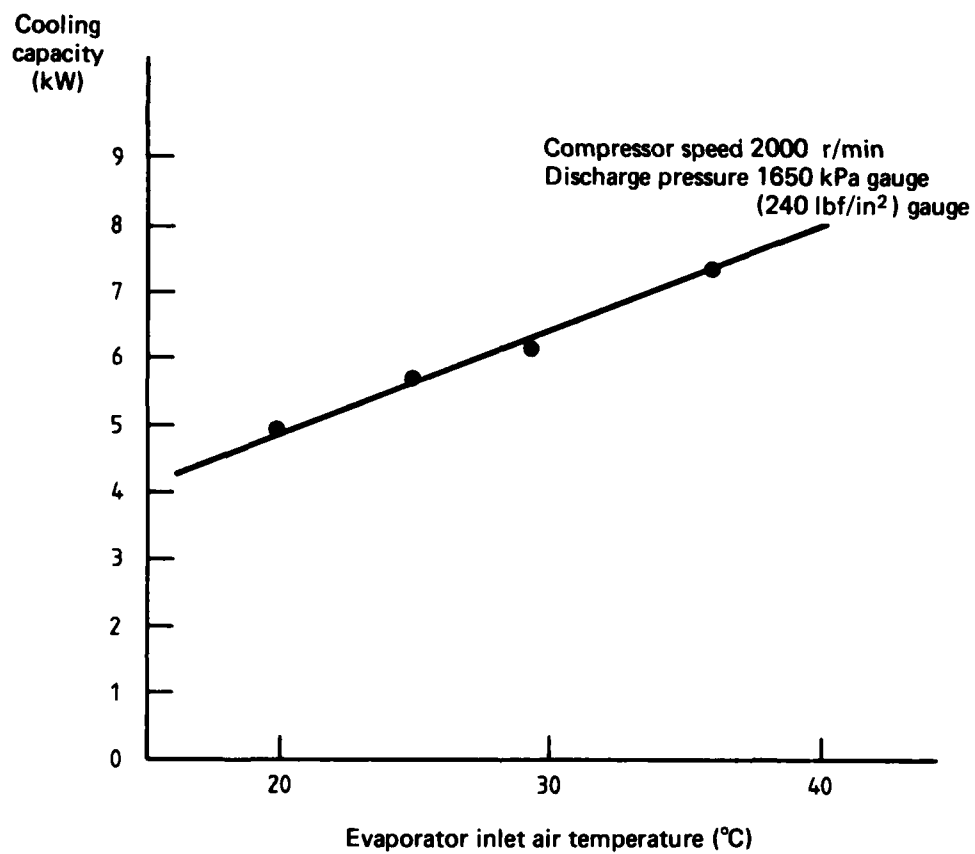
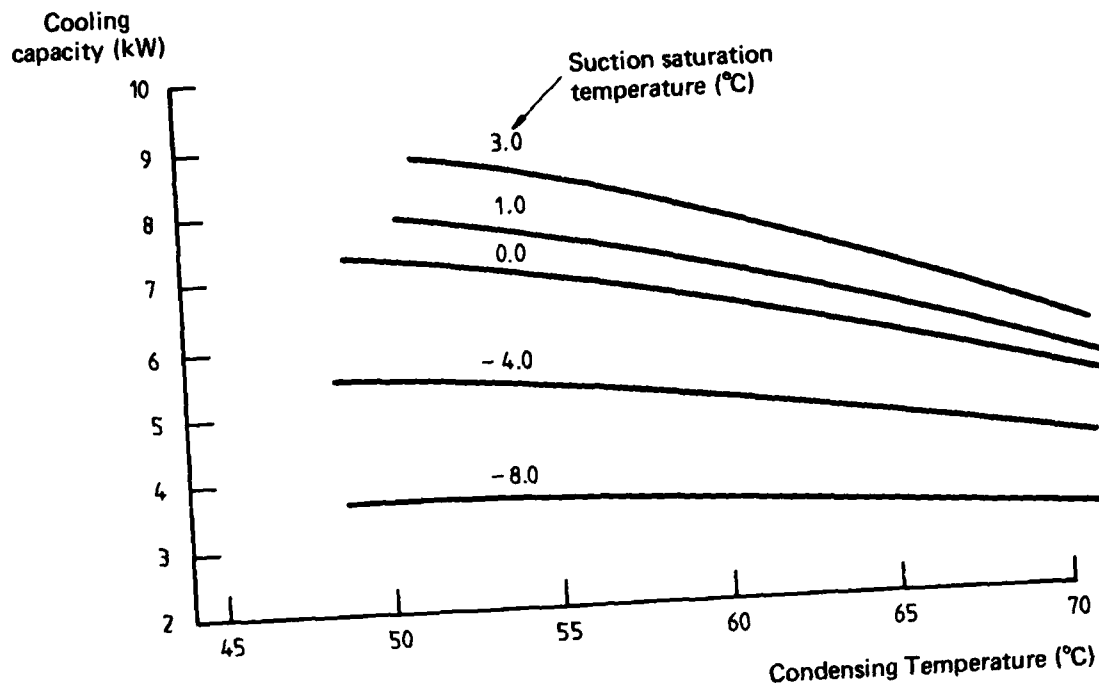
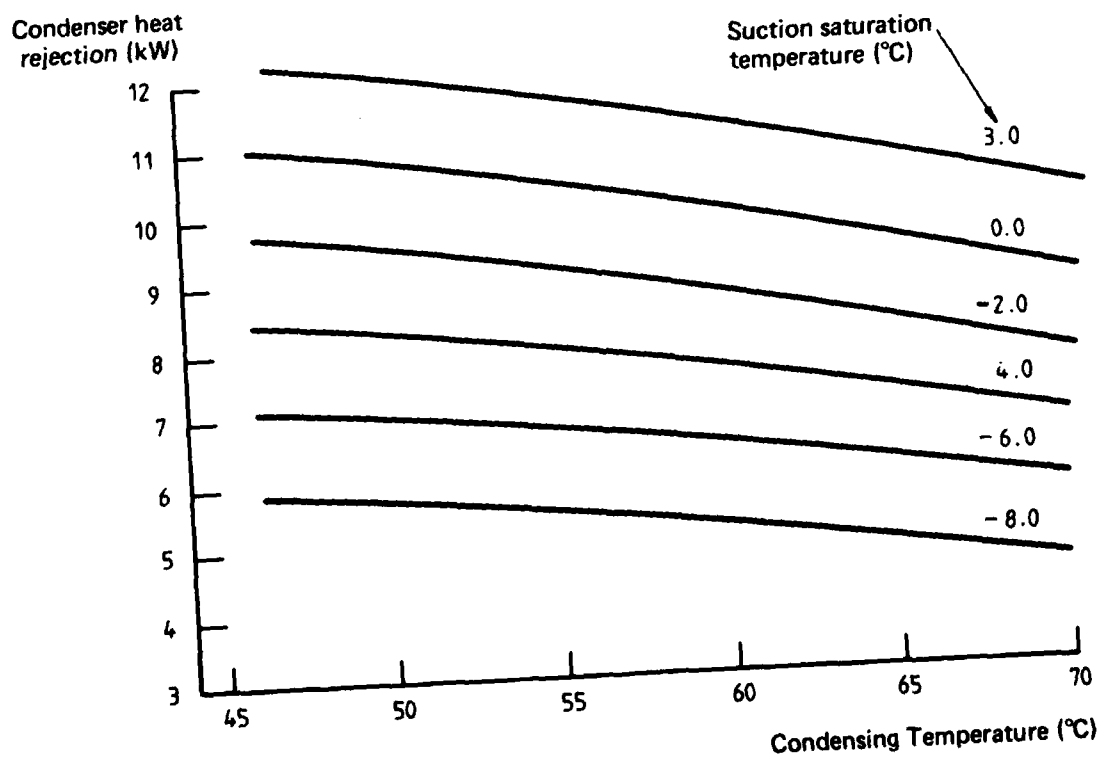


FIG. 22 EFFECT OF CHANGES IN EVAPORATOR INLET AIR TEMPERATURE
ON COOLING CAPACITY

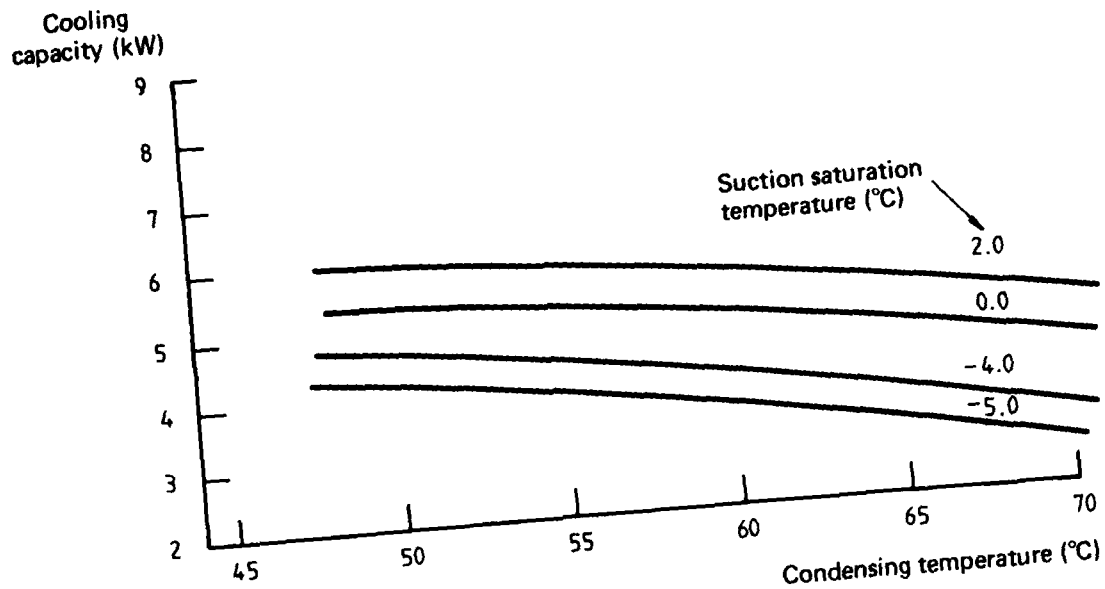


(a) Cooling capacity

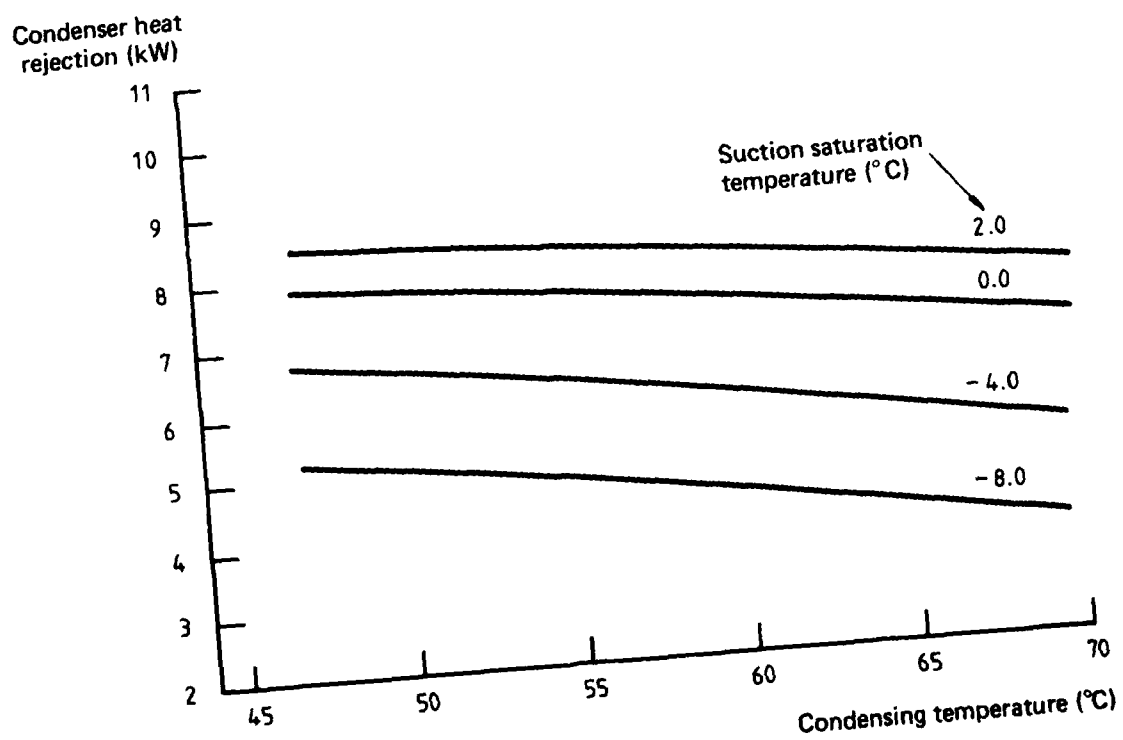


(b) Condenser heat rejection

FIG. 23a, b COMPRESSOR PERFORMANCE DIAGRAM, YORK 209 COMPRESSOR.
SPEED 3000 R/MIN, 6°C SUPERHEAT, 6°C SUBCOOLING

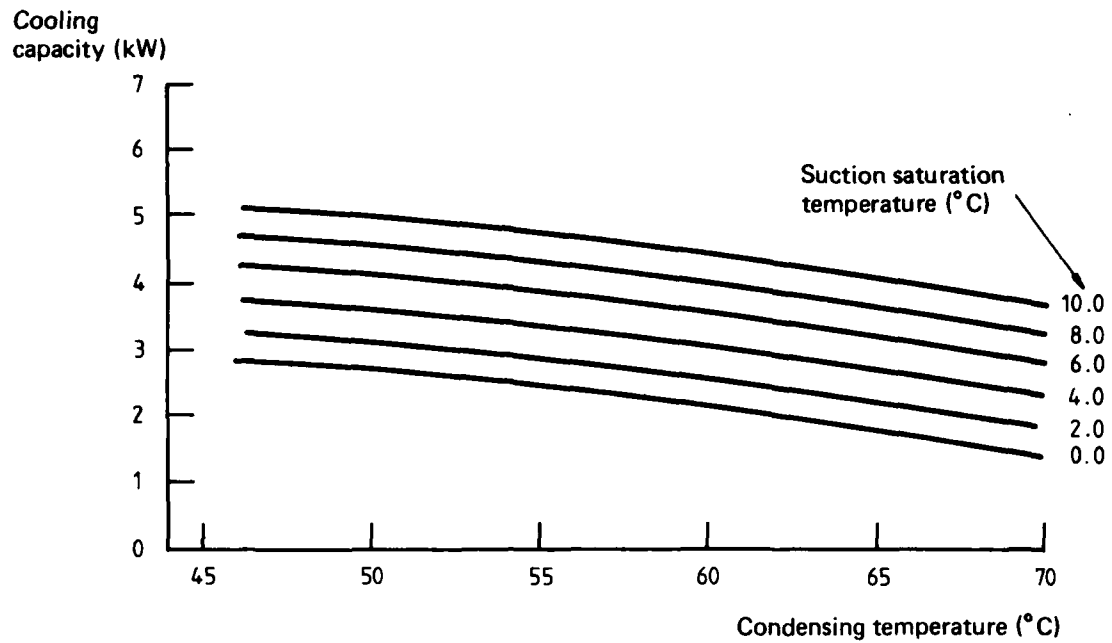


(a) Cooling capacity

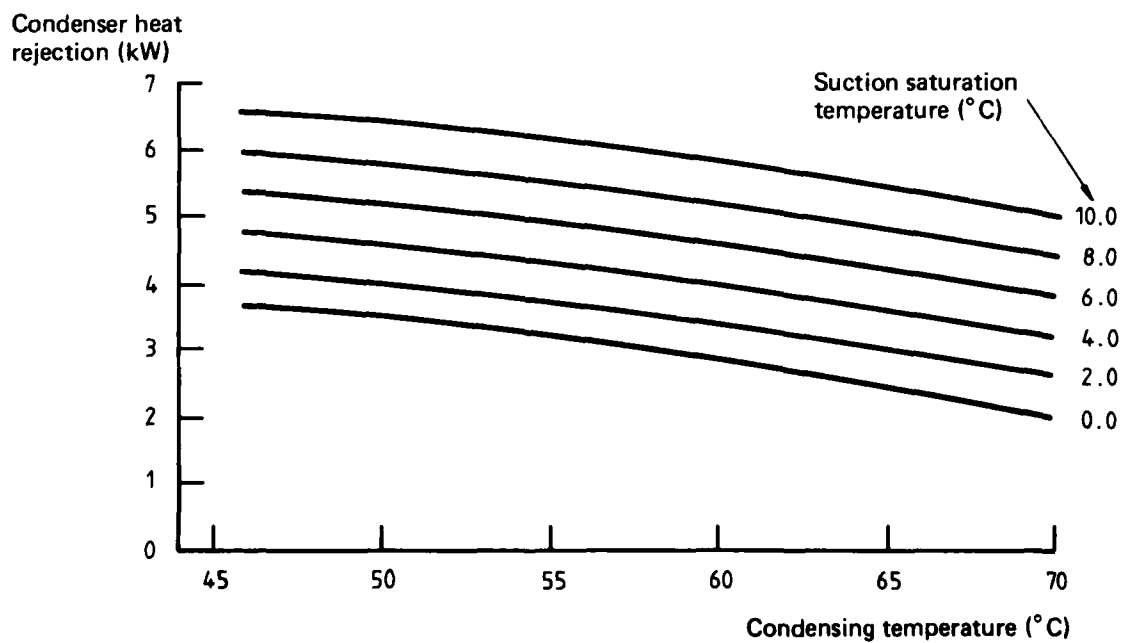


(b) Condenser heat rejection

FIG. 24a, b COMPRESSOR PERFORMANCE DIAGRAM, YORK 209, COMPRESSOR
SPEED 2000 R/MIN, 6°C SUPERHEAT, 6°C SUBCOOLING

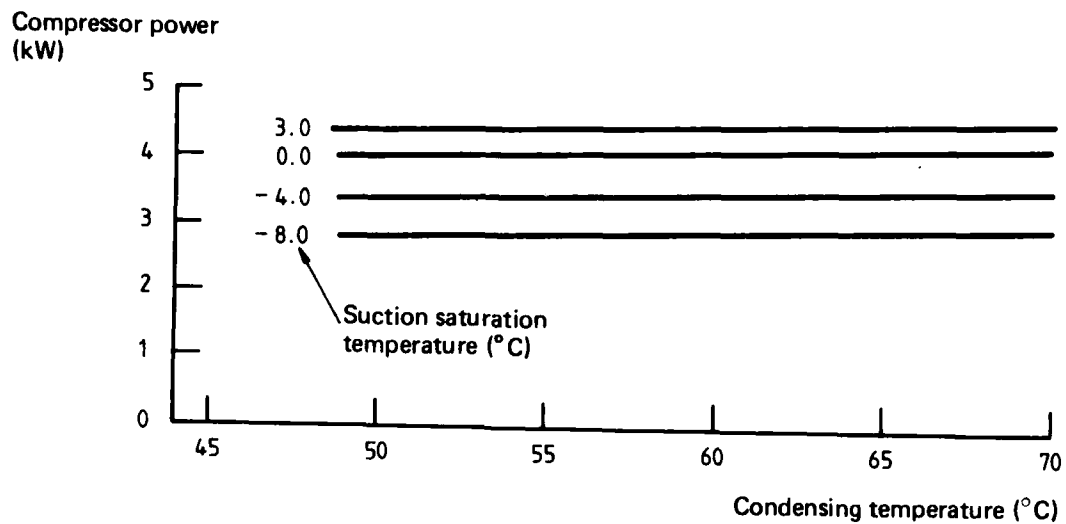


(a) Cooling capacity

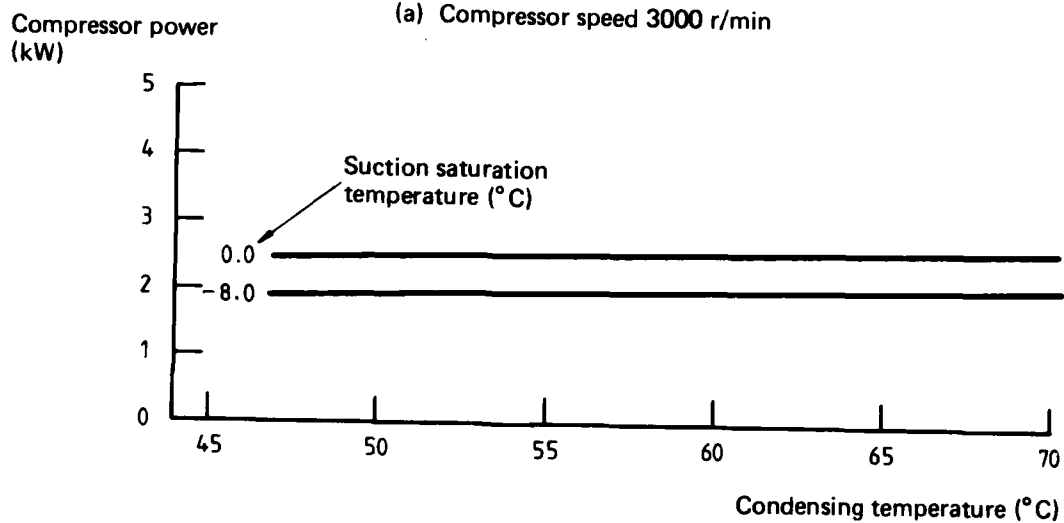


(b) Condenser heat rejection

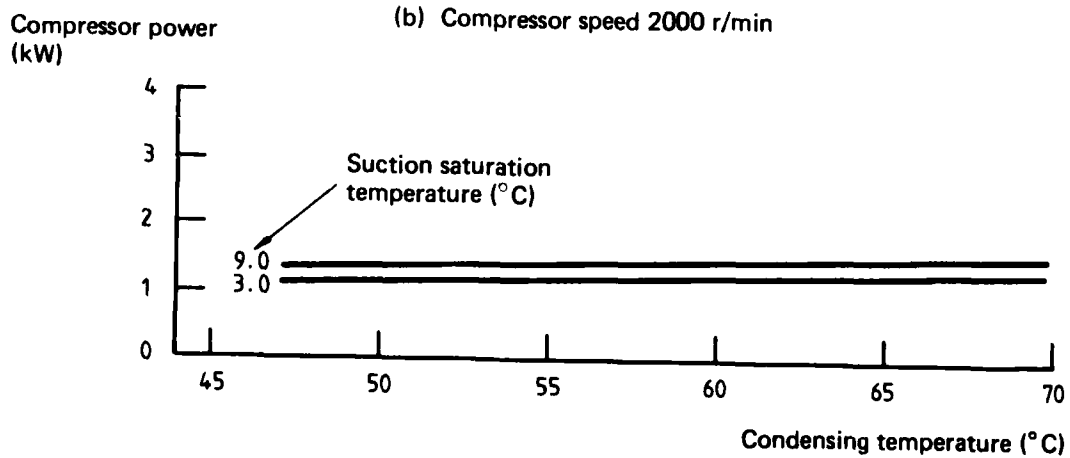
FIG. 25 a, b COMPRESSOR PERFORMANCE DIAGRAM YORK 209 COMPRESSOR.
SPEED 1000 R/MIN, 6°C SUPERHEAT, 6°C SUBCOOLING



(a) Compressor speed 3000 r/min



(b) Compressor speed 2000 r/min



(c) Compressor speed 1000 r/min

FIGS. 26 a, b, c COMPRESSOR POWER CONSUMPTION (YORK 209 COMPRESSOR)

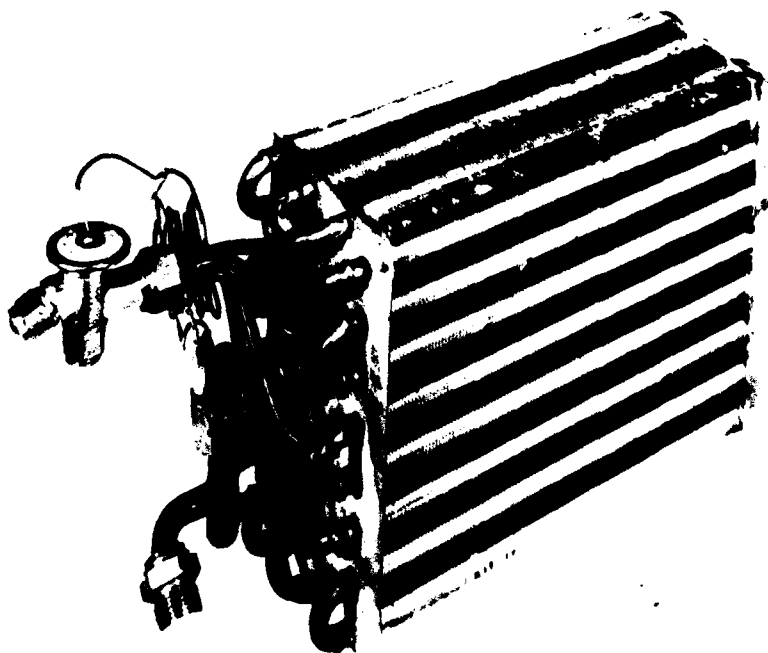
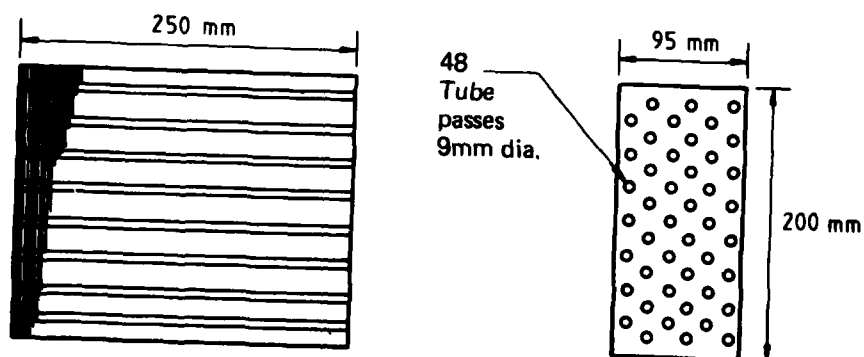


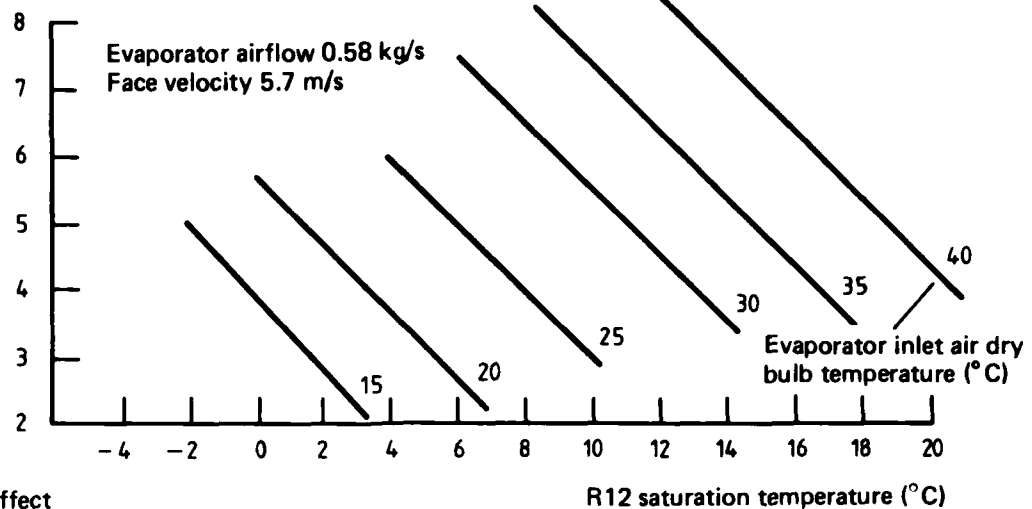
FIG. 27 (a) EVAPORATOR MATRIX



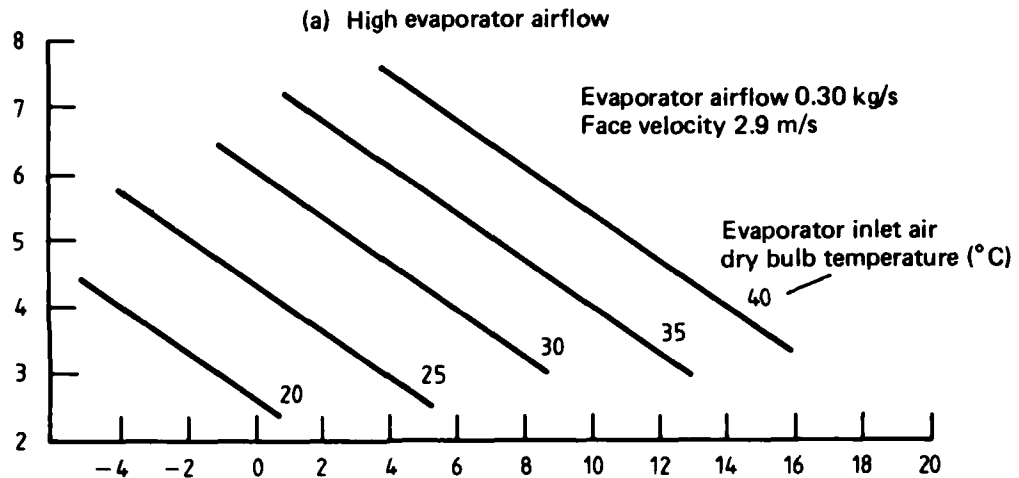
Weight: 3.20 kg (incl. T-X valve)

FIG. 27 (b) DIMENSIONS AND LAYOUT OF EVAPORATOR MATRIX

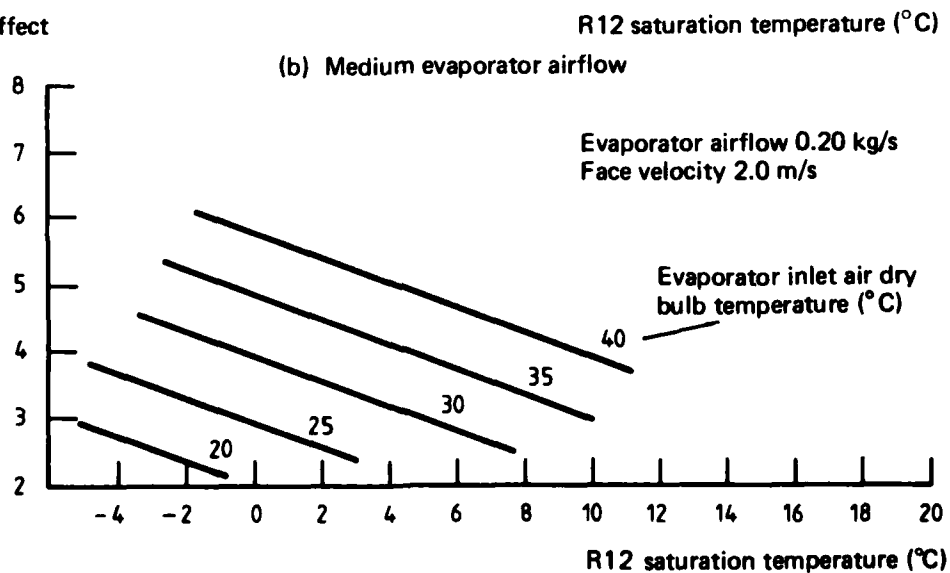
Cooling effect
(kW)



Cooling effect
(kW)



Cooling effect
(kW)



(c) Low evaporator airflow

FIGS. 28 a, b, c EVAPORATOR PERFORMANCE DIAGRAMS FOR TWO PARALLEL EVAPORATORS

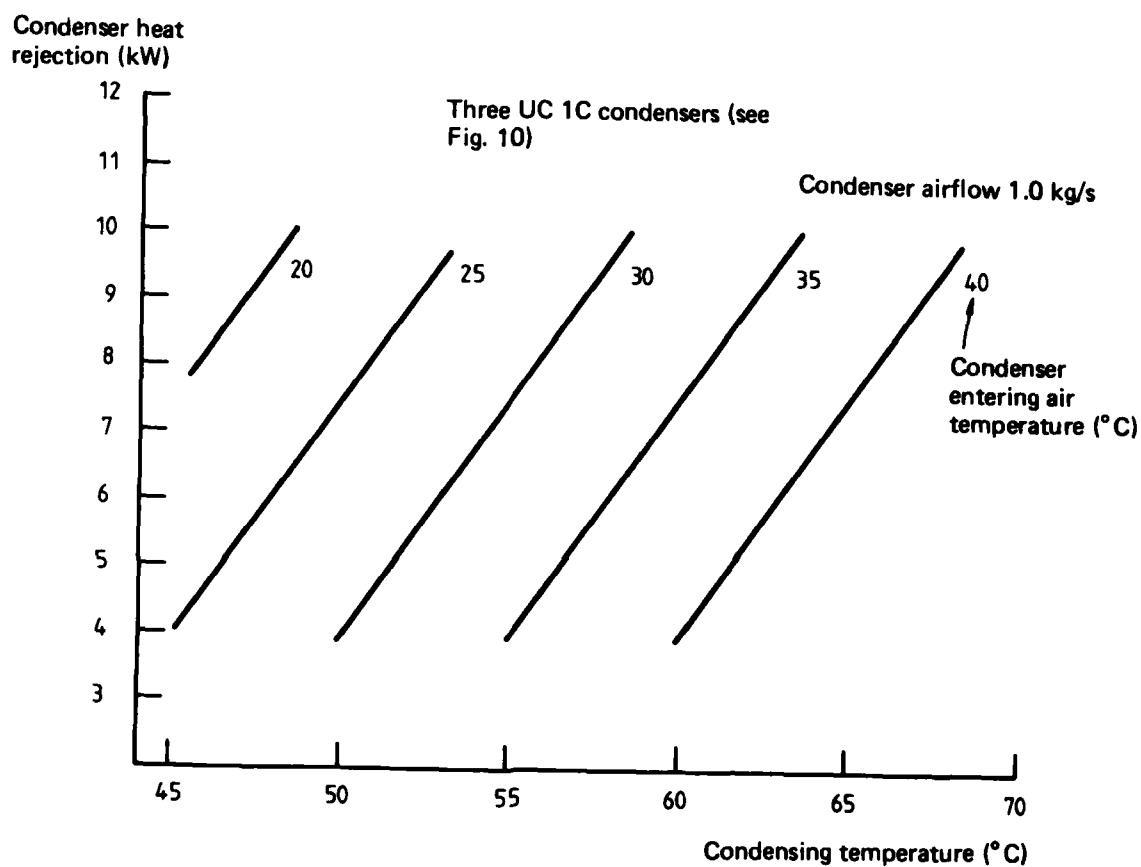


FIG. 29 CONDENSER PERFORMANCE DIAGRAM

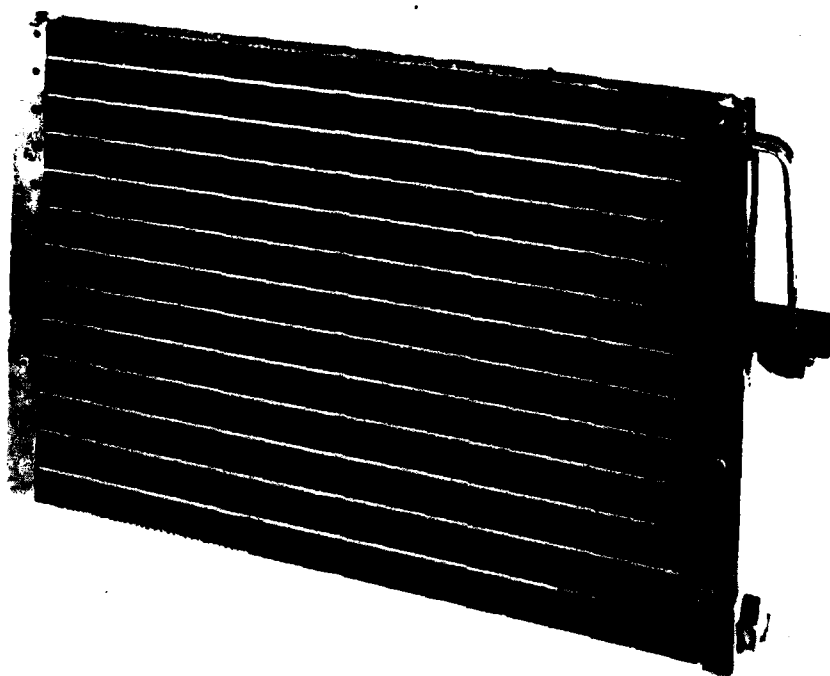
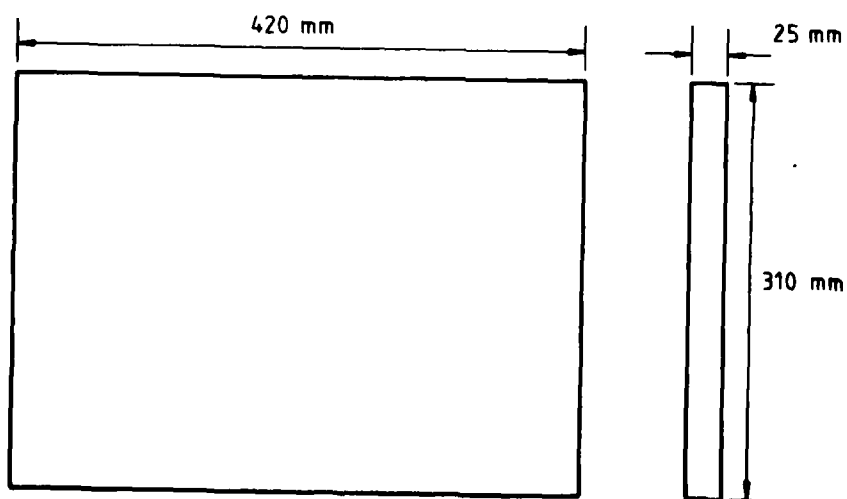


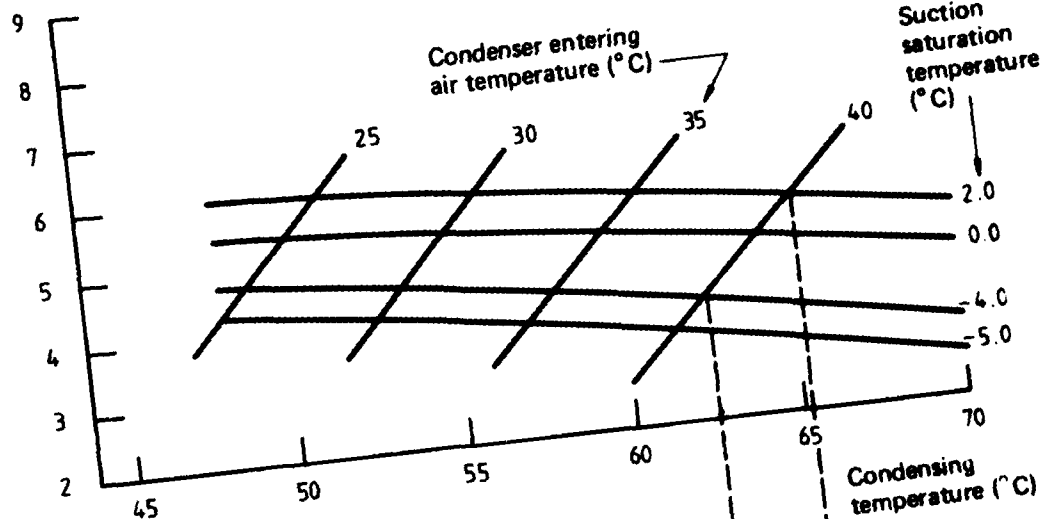
FIG. 30 a UC 1C CONDENSER



Weight: 2.50 kg

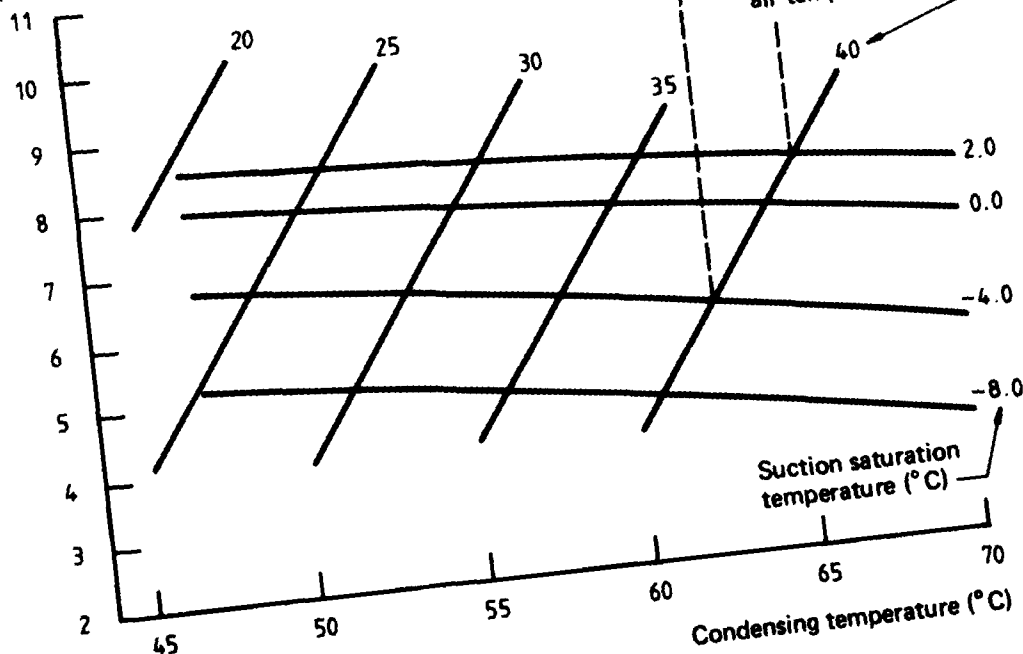
FIG. 30 b DIMENSIONS OF UC 1C CONDENSER

Cooling capacity
(kW)



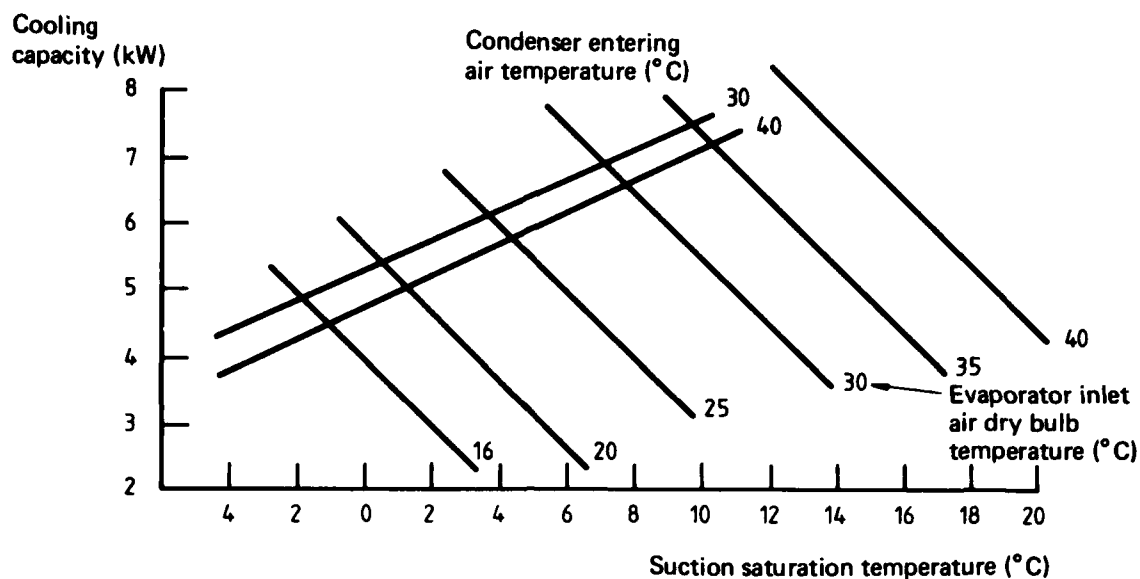
(a) Compressor

Condenser heat rejection (kW)

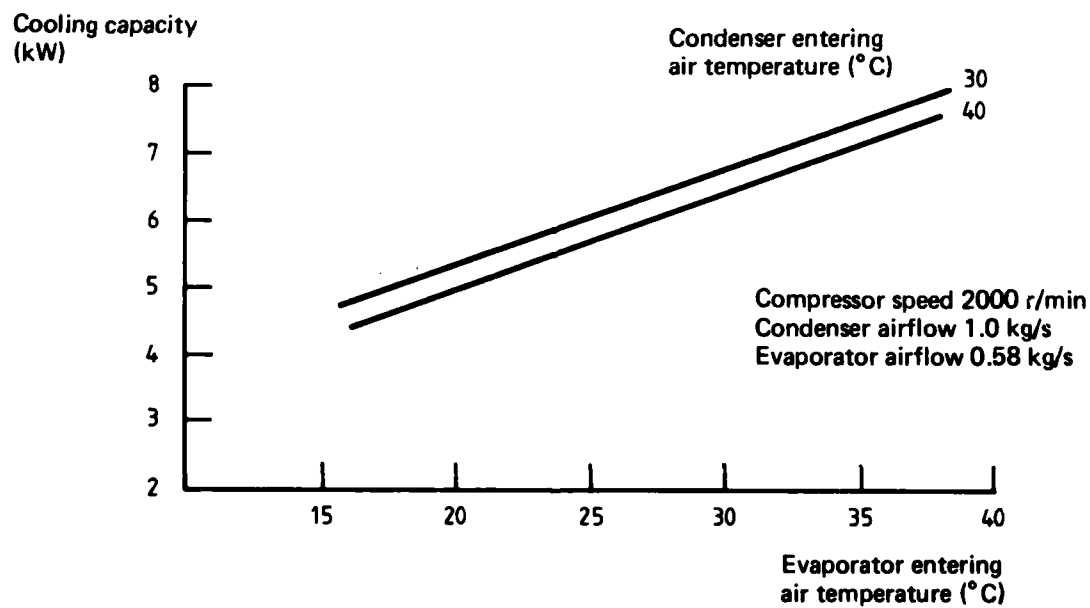


(b) Compressor and condenser

FIGS. 31 a, b COMBINED PERFORMANCE DIAGRAM FOR COMPRESSOR AND CONDENSER



(a) Plot of Fig. 31(a) onto Fig. 28(a)



(b) Overall system performance

FIGS. 32 a, b COMBINED PERFORMANCE DIAGRAM FOR OVERALL SYSTEM

DISTRIBUTION

AUSTRALIA

Copy No.

Department of Defence

Central Office

Chief Defence Scientist	1
Deputy Chief Defence Scientist	2
Superintendent, Science and Technology Programmes	3
Australian Defence Scientific and Technical Representative (UK)	—
Counsellor, Defence Science (USA)	—
Defence Central Library	4
Document Exchange Centre, DISB	5-21
Director General—Army Development (NCO)	22
Joint Intelligence Organisation	23

Aeronautical Research Laboratories

Chief Superintendent	24
Library	25
Superintendent—Mechanical Engineering Division	26
Division File—Mechanical Engineering	27
Authors: B. Rebbechi	28
J. L. Fowler	29
N. J. Repacholi	30
G. L. Collins	31
G. F. Pearce	32
Combustion Research Group	33

Materials Research Laboratories

Library	34
---------	----

Defence Research Centre

Library	35
---------	----

Central Studies Establishment

Information Centre	36
--------------------	----

RAN Research Laboratory

Library	37
---------	----

Victorian Regional Office

Library	38
---------	----

Navy Office

Naval Scientific Adviser	39
RAN Air Maintenance and Flight Trials Unit	40
Directorate of Naval Aircraft Engineering	41
Directorate of Naval Aviation Policy	42
Directorate of Naval Ship Design	43

Army Office

Army Scientific Adviser	44
Royal Military College Library	45
US Army Standardisation Group	46

Air Force Office		
Aircraft Research and Development Unit, Scientific Flight Group		47
Air Force Scientific Adviser		48
Technical Division Library		49
Director General Aircraft Engineering		50
Director General Operational Requirements		51
HQ Operational Command (SENGSO)		52
HQ Support Command (SENGSO)		53
RAAF Academy, Point Cook		54
Department of Industry and Commerce		
Government Aircraft Factories		
Manager		55
Library		56
Department of Transport		
Library		57
Statutory, State Authorities and Industry		
CSIRO, Mechanical Engineering Division, Library		58
Trans-Australia Airlines, Library		59
Gas & Fuel Corp. of Vic., Manager Scientific Services		60
SEC of Vic., Herman Research Laboratory, Library		61
Ansett Airlines of Australia, Library		62
Commonwealth Aircraft Corporation, Library		63
Hawker de Havilland Pty Ltd.:		
Librarian, Bankstown		64
Manager, Lidcombe		65
R. Jones		66
Rolls Royce of Australia Pty Ltd., Mr C. G. A. Bailey		67
Normalair-Garrett Ltd.		68
Marlандаire Pty. Ltd. (Melb.), Mr B. Humphreys		69
Mr R. E. Pavia		70
Universities and Colleges		
Adelaide	Barr Smith Library	71
La Trobe	Library	72
Melbourne	Engineering Library	73
	E. E. Milkins (Mechanical Eng.)	74
Monash	Hargrave Library	75
Newcastle	Library	76
New England	Library	77
Sydney	Engineering Library	78
New South Wales	Library	79
	Physical Sciences Library	80
	Prof. G. D. Segeant	81
Queensland	Library	82
Tasmania	Engineering Library	83
Western Australia	Library	84
RMIT	Library	85
	Mech. & Production Eng., Dr. H. Kowalski	86
CANADA		
International Civil Aviation Organization, Library		87
NRC:		
Division of Mechanical Engineering, Director		88
Gas Dynamics Laboratory, Mr R. A. Tyler		89

FRANCE		
ONERA, Library		90
GERMANY		
ZLDI		91
INDIA		
National Aeronautical Laboratory, Director		92
ITALY		
Fiat Co., Dr G. Gabrielli		93
JAPAN		
National Aerospace Laboratory, Library		94
NEW ZEALAND		
Transport Ministry, Airworthiness Branch, Library		95
Universities		
Canterbury	Library	96
	Prof. D. Stevenson, Mech. Eng.	97
SWEDEN		
Aeronautical Research Institute, Library		98
SWITZERLAND		
F - W (Swiss Federal Aircraft Factory)		99
UNITED KINGDOM		
Aeronautical Research Council (NPL), Secretary		100
CAARC, Secretary (NPL)		101
Royal Aircraft Establishment Bedford, Library		102
Military Vehicles and Engineering Establishment		103
National Engineering Laboratory, Superintendent		104
British Library, Lending Division		105
Motor Research Association, Director		106
British Aerospace:		
Kingston-upon-Thames, Library		107
Manchester Division, Library		108
Hatfield-Chester Division, Library		109
British Hovercraft Corporation Ltd., Library		110
Westland Helicopters Ltd.:		
Asst. Chief Designer Sea King		111
Chief Engineer		112
Normalair-Garrett Ltd.		113
Universities and Colleges		
Cranfield Inst. of Technology	Library	114
UNITED STATES OF AMERICA		
NASA Scientific and Technical Information Facility		115
Bell Helicopter Textron		116
Cessna Aircraft Co., Executive Engineer		117
Garrett Corporation		118
Hamilton Standard		119
Fairchild, Stratos Division		120
J. B. Systems Inc.		121
Boeing Vertol Company		122
Spares		123-132

END

DATE
FILMED

1-82

DTIC